DISCRETE AND CONTINUOUS
DYNAMICAL SYSTEMS SERIES B
Volume **8**, Number **4**, November **2007**

Website: http://aimSciences.org

pp. **801–831**

ANALYSIS OF A MODEL OF NUTRIENT DRIVEN SELF-CYCLING FERMENTATION ALLOWING UNIMODAL RESPONSE FUNCTIONS

Guihong Fan

Department of Mathematics and Statistics
McMaster University, Hamilton, Ontario L8S 4K1, CANADA

Gail S. K. Wolkowicz

Department of Mathematics and Statistics
McMaster University, Hamilton, Ontario L8S 4K1, CANADA

(Communicated by Linda Allen)

Abstract. A system of impulsive ordinary differential equations is used to model the growth of microorganisms in a self-cycling fermentor. The microorganisms are being used to remove a non-reproducing contaminant that is limiting to growth at both high and low concentrations. Hence it is the concentration of the contaminant that triggers the emptying and refilling process. This model predicts that either the process fails or the process cycles indefinitely with one impulse per cycle. Success or failure can depend on the choice of microorganisms, the initial concentration of the microorganisms and contaminant, as well as the choice for the emptying/refilling fraction. Either there is no choice of this fraction that works or there is an interval of possible choices with an optimal choice within the interval. If more than one strain is available, it does not seem to be the strains that have the highest specific growth rate over the largest range of the concentrations of the contaminant, but rather the ones that have the highest specific growth rate over very low concentrations of the contaminant, just above the threshold that initiates recycling that appear to be the most efficient, i.e., processing the highest volume of medium over a specified time period.

1. **Introduction.** Self-cycling fermentation (SCF) is a technique used to culture microorganisms. There are various potential applications, including water purification, waste decomposition, and production of antibiotics [9, 10, 13, 19, 21, 23, 26, 29].

SCF has been extensively described in [20, 21, 23], and thus only a brief review is needed here. The process is a computer-controlled semi-batch fermentation. A well-stirred tank containing fresh medium is initially inoculated with microorganisms. The microorganisms consume the nutrient until some criterion, sensed by the computer is met, (in the case studied in this paper, a particular concentration of the nutrient). The computer then initiates a rapid emptying and refilling process.

2000 *Mathematics Subject Classification.* Primary: 34K45, 34K60, 62P12; Secondary: 92D25, 92D40, 34D05.

Key words and phrases. Self-cycling fermentation, impulsive differential equations, nutrient driven process, tolerance, impulse time, emptying/refilling fraction, cycle time, optimal yield, bioremediation, water purification.

The second author's research is partially supported by NSERC and is the author to whom correspondence should be addressed.

A certain fraction of the contents of the tank is emptied and replaced by an equal volume of fresh medium. The process is then repeated. The process is considered successful if the fermentor cycles indefinitely, without human intervention, with reasonable cycle times (time between each successive recycling of the tank).

A mathematical model for SCF was developed in Wincure, Cooper, and Rey [27]. The response function describing the relationship between the limiting nutrient concentration and the growth rate of the microorganisms was modelled by a function of Monod form. They assumed the emptying/refilling process occurs instantaneously and used the dissolved oxygen concentration as the cycling criterion. Simulations based on their model predicted that the contents of the fermentor eventually oscillated in a stable periodic fashion, agreeing with their experimental results.

Smith and Wolkowicz [23] generalized the class of response functions to include any reasonable monotone increasing response function. They used a specified concentration of the contaminant as the triggering mechanism, and gave a mathematically rigorous analysis of a model that was formulated in terms of impulsive differential equations instead of Dirac Delta functions.

However, as has been pointed out by Powell [18], some reasonable response functions are not monotonically increasing, but rather unimodal, since some nutrients that limit growth at low concentrations are also inhibitory at high concentrations (see [4, 8, 16]). This is particularly true for microorganisms used in the treatment of biological or industrial waste or for water purification. In this paper, we generalize the model in [23] to allow response functions that are unimodal and assume throughout that the fermentor is being used to reduce some contaminant to a safe level and so use a safe concentration of the contaminant as the cycling criterion. Our analytic results are for general unimodal response functions. However, in the numerical simulations, we use functions determined by Alagappan and Cowan [3] to be the best fit for the particular strains and substrates involved (see Sections 3 and 4).

The analytic results predict that just as in the case of monotone response functions, three outcomes are possible. Either the process is successful and cycles indefinitely with a fixed cycle time (eventually), or it is unsuccessful and either terminates after a finite number of cycles, or it cycles indefinitely, but the cycle time becomes longer and longer, approaching infinity. Once an acceptable level of contaminant is set, whether or not the process is successful, depends on the relative values of certain species specific parameters and can be initial condition dependent. The emptying/refilling fraction also has an important impact. The dynamics of the model are not sensitively dependent on the form of the response function. This would seem to indicate that the potential of the model for prediction is very robust. However, there are extra considerations required if the response functions are unimodal rather than monotone increasing.

This paper is organized as follows. In Section 2, we formulate the model and then provide criteria that predict whether or not the process will be successful and if not how it will fail. Simulations illustrating successful operation in the case of biodegradation of toluene by the strain Ralstonia picketti PKO1 are provided in Section 3. In Section 4, we conclude that once a strain of microorganisms is chosen and the threshold for initiating the emptying and refilling process is set, there is an open interval of feasible choices for the emptying and refilling fraction. However, this interval could be empty. Within the interval, if it is nonempty,

there is an optimal choice that gives the optimal output over a given time period. Using an explicit formula for the cycle time we discuss the selection of the optimal emptying/refilling fraction and illustrate how to do this in the case of several strains of microorganisms. We also compare the efficiency of several strains that degrade the contaminant, toluene. In Section 5, we provide rigorous proofs of our main results and we conclude in Section 6 with a discussion of the potential implications for applications.

2. A nutrient driven model for the self-cycling fermentation process.

2.1. **The model.** In this section we generalize the model for the nutrient driven self-cycling fermentation process studied by Smith and Wolkowicz [23] to allow for substrates that are limiting at both low and high concentrations. Since the time taken to empty and refill the tank is negligible compared to each cycle time, we assume that the emptying and refilling process occurs instantaneously, and as in [23] formulate the model as a system of impulsive differential equations.

Impulsive differential equations are described in Bainov and Simeonov [5, 6, 7] and Lakshmikantham, Bainov, and Simeonov [15]. Using the standard notation for impulsive differential equations (see [5, 6]), for a given function $y(t)$, and time τ,

$$\Delta y \equiv y^+ - y^-,$$

where

$$y^+ \equiv y(\tau^+) \equiv \lim_{t\to\tau^+} y(t) \quad \text{and} \quad y^- \equiv y(\tau^-) \equiv \lim_{t\to\tau^-} y(t).$$

The model of nutrient driven self-cycling fermentation takes the form of the following system of impulsive differential equations:

$$\begin{array}{rcll} \dfrac{dx}{dt} &=& -\bar{d}x + f(s)x, & s \neq \bar{s}, \\ \dfrac{ds}{dt} &=& -\dfrac{1}{Y}f(s)x, & s \neq \bar{s}, \\ \Delta x &=& -rx^-, & s = \bar{s}, \\ \Delta s &=& -r\bar{s} + rs^i, & s = \bar{s}, \end{array} \tag{1}$$

$$x(0) > 0,\ s(0) > \bar{s}.$$

Here, t denotes time in minutes, s denotes the concentration (g/L) of the limiting nutrient in the fermentor as a function of t, x the biomass concentration (g/L) of the population of microorganisms that consume the nutrient (also as a function of t), Y the cell yield constant (g biomass/g limiting substrate), $\bar{d}$ the species-specific death rate (per minute), s^i the concentration (g/L) of the fresh medium added to the tank at the beginning of each new cycle, $\bar{s}$ the threshold concentration (g/L) of limiting nutrient that triggers the emptying and refilling process, and r the emptying/refilling fraction. It is assumed that $\bar{d} \geqslant 0$, $Y > 0$, $s^i > \bar{s} > 0$, and $0 < r < 1$.

The response function f is assumed to satisfy:

$$\begin{array}{ll} \text{i.} & f : \mathbb{R}_+ \to \mathbb{R}_+; \\ \text{ii.} & f \text{ is continuously differentiable;} \\ \text{iii.} & f(0) = 0,\ f(s) > 0 \text{ for } s > 0; \\ \text{iv.} & \text{There exists } M > 0 \text{ such that } f'(s) > 0 \text{ for } 0 < s < M, \\ & \text{and } f'(s) < 0 \text{ for } s > M, \text{ where } M = \infty \text{ is possible.} \end{array} \tag{2}$$

It is assumption (iv) that allows the response function to be inhibitory at high concentrations of the nutrient. However, if the response function is monotone increasing, then $M = \infty$, and the model is precisely the one considered in [23].

Let t_k denote the time at which the concentration of the limiting nutrient in the tank reaches the specified threshold, $\bar{s}$, for the kth time, called the kth moment of impulse or impulse time. Hence, $s(t_k^-) = \bar{s}$. From (1), it follows that $\Delta x(t_k) = x(t_k^+) - x(t_k^-) = -rx(t_k^-)$, and so $x(t_k^+) = (1-r)x(t_k^-)$, and $\Delta s(t_k) = s(t_k^+) - s(t_k^-) = -r\bar{s} + rs^i$, and so $s(t_k^+) = (1-r)\bar{s} + rs^i$. For convenience, we define

$$\bar{s}^+ \equiv (1-r)\bar{s} + rs^i.$$

Since $s(t)$ decreases during each cycle, if $s(0) < \bar{s}$, the tolerance $\bar{s}$ is never reached and the process fails. It is assumed that $s(0) \neq \bar{s}$, to avoid an immediate impulsive effect. In the applications we have in mind, such as water purification or waste decomposition, s^i would denote the concentration of some contaminant in the environment, $s(t)$ the concentration of the contaminant in the fermentation tank, and $\bar{s}$ the acceptable level of the contaminant in the environment, consistent with standards set by an environmental protection agency. For such applications, normally $s(0) = s^i$.

Define parameters $0 \leqslant \lambda \leqslant \mu$ (possibly infinity) to be the *break-even* concentrations of the nutrient, i.e., $f(\lambda) = \bar{d}$, $f(\mu) = \bar{d}$, since $x'(t) = 0$ if $s(t)$ is equal to either one of these concentrations. The biomass concentration of the microorganism population increases only if $\lambda < s(t) < \mu$. If f is bounded below $\bar{d}$, then we define $\lambda, \mu = \infty$ and there is no hope for the process to succeed. If $f(s) > \bar{d}$ for all $s > \lambda$, then $\mu = \infty$.

If $\bar{s}^+ < \mu$ and $s(0) < \mu$, the global analysis given in Smith and Wolkowicz [23] applies and the dynamics are already completely understood. Here, we are therefore especially interested in the case that $\bar{s} < \mu < \bar{s}^+$.

2.2. **The associated system of ordinary differential equations.** Between impulses the system is modelled by a system of ordinary differential equations. This system will be called the associated system of ordinary differential equations and is given by

$$\begin{aligned} \frac{dx}{dt} &= -\bar{d}x + f(s)x, \\ \frac{ds}{dt} &= -\frac{1}{Y}f(s)x, \\ x(0) \geqslant 0,\ s(0) &\geqslant 0. \end{aligned} \tag{3}$$

For our analysis it is necessary to understand the dynamics of this associated system for a slightly expanded set of initial conditions compared to system (1). Figure 1 depicts typical phase portraits in x-s space, in the case a) that $\bar{d} = 0$ and b) that $\bar{d} > 0$. Using standard phase portrait analysis, it is easy to show that solutions of (3) remain nonnegative and bounded.

If $\bar{d} = 0$, then $\lambda = 0$ and $\mu = \infty$. In this case, all points of the form $(0, s^*)$ with $s^* \geqslant 0$ and $(x^*, 0)$ with $x^* \geqslant 0$ are equilibrium points. See Figure 1 a). All orbits lie along lines $Ys + x = Ys(0) + x(0)$ with $x(t)$ increasing and $s(t)$ decreasing. Any orbit with initial conditions satisfying $x(0) > 0$, $s(0) > 0$, approaches $(x^*, 0)$, where $x^* = Ys(0) + x(0) > 0$ and hence, all equilibrium points of this form are stable (but not asymptotically stable). All equilibrium points of the form $(0, s^*)$, with $s^* > 0$ are unstable.

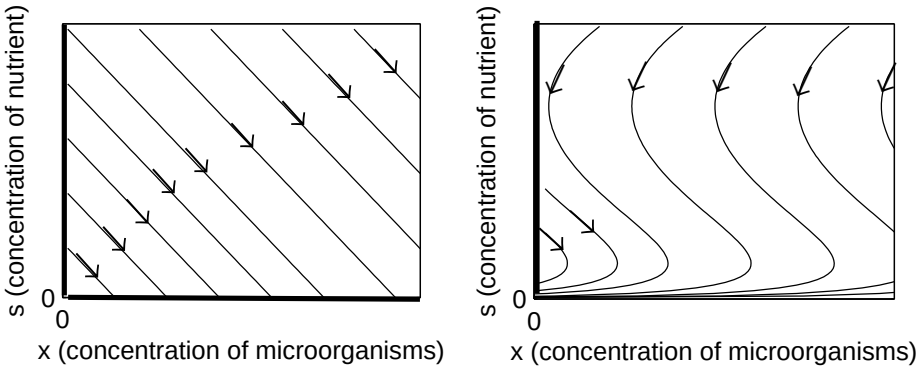

FIGURE 1. Phase portraits for the associated ordinary differential equations (3). The bold lines on the axes consist of equilibrium points. (LEFT) Phase portrait with $\bar{d} = 0$. All equilibrium points on the x-axis are stable but not asymptotically stable. All equilibria on the s-axis are unstable except the origin. (RIGHT) Phase portrait with $\bar{d} > 0$. The concentration of microorganisms increases for $s \in (\lambda, \mu)$ and decreases if $s < \lambda$ or $s > \mu$. For all orbits of (3) starting in first quadrant, $x(t) \to 0$ as $t \to \infty$. The equilibrium points on the s-axis are stable for $s > \mu$ and $0 \leqslant s \leqslant \lambda$ and unstable for $\lambda < s \leqslant \mu$.

If $\bar{d} > 0$, then only points of the form $(0, s^*)$, with $s^* \geqslant 0$ are equilibrium points. See Figure 1 b). If $s^* > \mu$ or $s^* \leqslant \lambda$, then $(0, s^*)$ is stable, but not asymptotically stable. If $\lambda < s^* \leqslant \mu$, then $(0, s^*)$ is unstable. If $x(0) > 0$ and $s(0) > 0$, then $s(t)$ is decreasing for all time t and $x(t)$ increases for $\lambda < s(t) < \mu$, and decreases for $s(t) < \lambda$ or $s(t) > \mu$. Thus $(x(t), s(t))$ converges to an equilibrium point of the form $(0, s^*)$ with $s^* \geqslant \mu$ or $s^* < \lambda$, depending on the initial conditions.

Provided $x(0) > 0$ and $s(0) > 0$, from (3),

$$\frac{dx}{ds} = Y\left(\frac{\bar{d}}{f(s)} - 1\right), \tag{4}$$

a separable differential equation. It follows that

$$x(t) = x(0) + Y\int_{s(t)}^{s(0)} \left(1 - \frac{\bar{d}}{f(u)}\right)\, du. \tag{5}$$

It is useful to note that, the slope of trajectories of (4) depends only on s. Therefore, if $\tilde{\gamma}(t)$ and $\hat{\gamma}(t)$ are two orbits with initial conditions, $(\tilde{x}(0), \tilde{s}(0))$ and $(\hat{x}(0), \hat{s}(0))$, respectively, with $\tilde{s}(0) = \hat{s}(0)$, but $\tilde{x}(0) - \hat{x}(0) = \eta > 0$, then for any times $\tilde{t} > 0$ and $\hat{t} > 0$, where $\tilde{s}(\tilde{t}) = \hat{s}(\hat{t})$, it follows that $\tilde{x}(\tilde{t}) - \hat{x}(\hat{t}) = \eta$. Hence, once one orbit is known, then all others are just translations. It can also be shown that $\tilde{t} < \hat{t}$, and so although the orbits are translations, orbits starting with higher concentrations of the microorganism, i.e., further to the right, take less time to reduce the level of the contaminant.

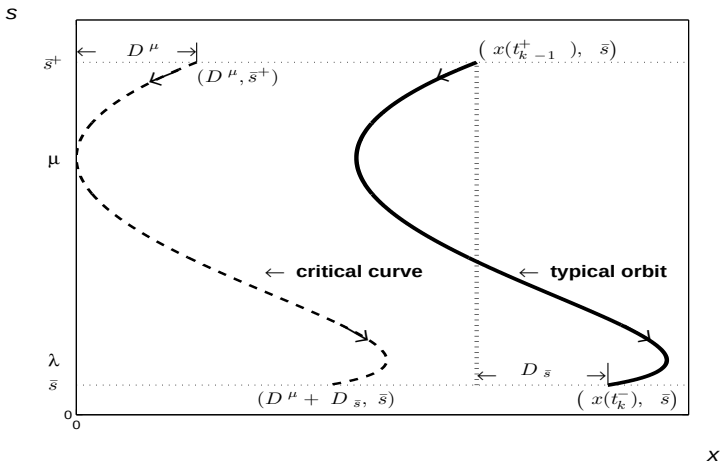

FIGURE 2. This graph, in phase space, shows the critical curve and a typical orbit of the associated ordinary differential equation that corresponds to a single cycle of the impulsive system (solid curve). The critical curve (dashed curve) consists of three orbits: the stable manifold of the equilibrium point $(0, \mu)$; the equilibrium point $(0, \mu)$; and the unstable manifold of the equilibrium point orbit $(0, \mu)$. D^μ is the distance from where the critical curve intersects the horizontal line $s = \bar{s}^+$ and the s axis. If $\bar{s}^+ \leqslant \mu$, then $D^\mu = 0$. If $s(0) = \bar{s}^+$ and $s(t) = \bar{s}$, then $D_{\bar{s}} = x(t) - x(0)$. Whenever, impulse times t_k and t_{k-1} are defined, $D_{\bar{s}} = x(t_k^-) - x(t_{k-1}^+)$.

2.3. **Dynamics of model (1).** We begin by defining,

$$D_{\bar{s}} \equiv Y \int_{\bar{s}}^{\bar{s}^+} \left(1 - \frac{\bar{d}}{f(s)}\right) ds, \tag{6}$$

$$D^\mu \equiv \begin{cases} 0, & \bar{s}^+ \leqslant \mu, \\ Y \int_{\bar{s}^+}^{\mu} \left(1 - \frac{\bar{d}}{f(s)}\right) ds, & \bar{s}^+ > \mu. \end{cases}$$

Since $f(s) < \bar{d}$ for $s > \mu$, we have $D^\mu > 0$ for $\bar{s}^+ > \mu$. So $D^\mu \geqslant 0$ in both cases. The relative values of $D_{\bar{s}}$ and D^μ will play an important role in our results.

If $s(0) = \bar{s}^+$ and $s(t) = \bar{s}$ in (5), it follows that $x(t) - x(0) = D_{\bar{s}}$. Therefore, whenever impulse times t_{k-1} and t_k are defined,

$$x(t_k^-) - x(t_{k-1}^+) = D_{\bar{s}} \tag{7}$$

is constant (see Figure 2).

We define a "critical curve" to be the curve consisting of three orbits: the stable manifold of the equilibrium point $(0, \mu)$; the equilibrium point $(0, \mu)$; and the unstable manifold of the equilibrium point $(0, \mu)$. In Figure 2 the unstable manifold of the equilibrium point $(0, \mu)$ intersects the horizontal line $s = \bar{s}$ at $x = D^\mu + D_{\bar{s}}$. This is always the case if $D_{\bar{s}} + D^\mu \geqslant 0$. However, if $D_{\bar{s}} + D^\mu < 0$, it does not reach the horizontal line $s = \bar{s}$, but rather converges to an equilibrium of the form $(0, s^*)$ where $\bar{s} < s^* < \lambda$.

D^μ is the distance from where the critical curve intersects the horizontal line $s = \bar{s}^+$ and the s axis. The significance of the critical curve will become more apparent subsequently.

In the remainder of this section we present three theorems that predict the dynamics of model (1) in the cases not already considered in [23]. Unless otherwise stated, we assume that $\bar{d} > 0$. The proofs are given in Section 5. First we characterize when a periodic orbit exists and describe the periodic orbit.

Definition 2.1. A periodic orbit $\gamma(t)$ has the *property of asymptotic phase* if for each point y in the basin of attraction of the periodic orbit, there exists a unique $\theta(y)$ such that $\lim_{t\to\infty} |y(t) - \gamma(t + \theta(y))| = 0$, where $y(t)$ is the solution through the point y.

Theorem 2.2. *Consider model (1) with $\bar{s} < \mu < \bar{s}^+$. There exists a nontrivial positive periodic orbit if and only if $\frac{1-r}{r} D_{\bar{s}} > D^\mu$. The periodic orbit is unique and has exactly one impulse per period, is asymptotically stable, and has the property of asymptotic phase.*

At the impulse times $\{t_n\}_{n=1}^\infty$, the periodic orbit satisfies

$$\begin{array}{rclcrcl} x(t_n^-) & = & \frac{1}{r} D_{\bar{s}}, & & x(t_n^+) & = & \frac{1-r}{r} D_{\bar{s}}, \\ s(t_n^-) & = & \bar{s}, & & s(t_n^+) & = & \bar{s}^+. \end{array}$$

The period of the periodic orbit is given by:

$$T = \int_{\bar{s}}^{\bar{s}^+} \frac{Y}{f(s)} \left(\frac{1}{\frac{(1-r)}{r} D_{\bar{s}} + Y \int_s^{\bar{s}^+} \left(1 - \frac{\bar{d}}{f(u)}\right) du} \right) ds.$$

From Theorem 2.2 it follows immediately that if $D_{\bar{s}} \leqslant 0$ then no periodic orbit exists and the process fails. However, if $D_{\bar{s}} > 0$, then it may be possible to find a range of values of the emptying and refilling fraction $r \in (0, 1)$ for which $\frac{1-r}{r} D_{\bar{s}} > D^\mu$. In this case a locally asymptotically stable periodic orbit exists (see the solid orbit in Figure 3 (TOP)). As will be shown in Theorem 2.3, at least in theory, the process is successful, provided the initial conditions are chosen appropriately.

In order to understand how the initial conditions affect the predicted outcome, first notice that if $\frac{1-r}{r} D_{\bar{s}} = D^\mu$, it follows that

$$\frac{D_{\bar{s}}}{r} = D^\mu + D_{\bar{s}} = D^\mu + \frac{r}{1-r} D^\mu = \frac{D^\mu}{1-r}.$$

A similar result holds if one replaces "=" everywhere by ">" or by "<". Therefore, one and only one of the following holds: either

i) $\frac{1-r}{r} D_{\bar{s}} > D^\mu \iff \frac{D_{\bar{s}}}{r} > D^\mu + D_{\bar{s}} > \frac{D^\mu}{1-r}$ (see Figure 3 (TOP)), or

ii) $\frac{1-r}{r} D_{\bar{s}} = D^\mu \iff \frac{D_{\bar{s}}}{r} = D^\mu + D_{\bar{s}} = \frac{D^\mu}{1-r}$ (Figure 3 (MIDDLE)), or

iii) $\frac{1-r}{r} D_{\bar{s}} < D^\mu \iff \frac{D_{\bar{s}}}{r} < D^\mu + D_{\bar{s}} < \frac{D^\mu}{1-r}$ (Figure 3 (BOTTOM)).

The following three conditions will prove useful to describe how the initial conditions affect the outcome in model (1).

(A_1) $x(0) + Y \int_{\bar{s}}^{s(0)} \left(1 - \frac{\bar{d}}{f(s)}\right) ds > 0,$

(A_2) $x(0) + Y \int_{\mu}^{s(0)} \left(1 - \frac{\bar{d}}{f(s)}\right) ds > 0,$

(A_3) $(1 - r)\left(x(0) + Y \int_{\bar{s}}^{s(0)} \left(1 - \frac{\bar{d}}{f(s)}\right) ds\right) > D^\mu.$

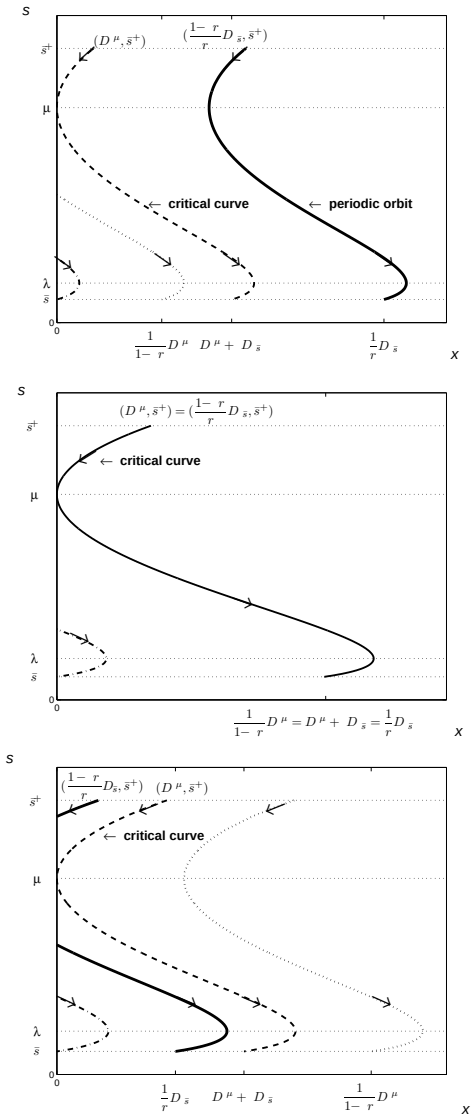

FIGURE 3. The relative positions (in phase space) of the periodic orbit and the critical curve when: (TOP) $\frac{1}{1-r}D^\mu < D^\mu + D_{\bar{s}} < \frac{1}{r}D_{\bar{s}}$. There is a unique attracting periodic orbit; (MIDDLE) $\frac{1}{1-r}D^\mu = D^\mu + D_{\bar{s}} = \frac{1}{r}D_{\bar{s}}$. No periodic orbit exists. The dashed, dotted, and solid curves above coalesce forming the critical curve; (BOTTOM) $\frac{1}{r}D_{\bar{s}} < D^\mu + D_{\bar{s}} < \frac{1}{1-r}D^\mu$. Again no periodic orbit exists. The dotted curve in the top graph now sits to the right side of the critical curve and the solid curve sits to the left (possibly totally disappearing if made up completely of negative values). In all three cases: if $\lambda < \bar{s}$, then the dash-dotted curve no longer exists; if $\bar{s}^+ \leqslant \mu$, then $D^\mu = 0$ and the dotted curve disappears.

Note that, since $D^\mu \geqslant 0$, (A_3) implies (A_1).

Orbits that have initial conditions satisfying

$$x(0) + Y \int_{\bar{s}}^{s(0)} \left(1 - \frac{\bar{d}}{f(s)}\right) ds = 0$$

lie on the stable manifold of the equilibrium point $(0, \bar{s})$ (see the dash-dotted curve at the bottom left of each graph in Figure 3.) Any orbit that starts inside the region bounded by this stable manifold and the s-axis never reaches $\bar{s}$, but rather converges to an equilibrium of the form $(0, s^*)$ where $\bar{s} < s^*$, and so there are no impulses. If (A_1) holds, the orbit starts outside this region. If $\lambda < \bar{s} < \mu$, then the equilibrium point $(0, \bar{s})$ is unstable and this region is empty.

Orbits that have initial conditions satisfying

$$s(0) > \mu \quad \text{and} \quad x(0) + Y \int_{\mu}^{s(0)} \left(1 - \frac{\bar{d}}{f(s)}\right) ds = 0$$

lie on the stable manifold of the equilibrium point $(0, \mu)$ (see the dashed curve above the horizontal line $s = \mu$ in each graph in Figure 3). For any orbit that initiates inside the region bounded by this curve and the s-axis, $s(t)$ never reaches μ, but rather converges to an equilibrium of the form $(0, s^*)$ with $s^* > \mu$. If (A_2) is satisfied, then the orbit starts in the region to the right of this portion of the dashed curve.

Orbits that have initial conditions satisfying

$$(1 - r)\left(x(0) + Y \int_{\bar{s}}^{s(0)} \left(1 - \frac{\bar{d}}{f(s)}\right) ds\right) = D^\mu$$

are depicted in Figure 3 by the dotted curves. In Figure 3 (MIDDLE) this curve coalesces with the *critical curve* and the periodic orbit. (This is the motivation for the nomenclature.) For orbits with initial conditions on this curve, there is a time t_1 satisfying $s(t_1^-) = \bar{s}$. The corresponding value, $x(t_1^-) = \frac{1}{1-r} D^\mu$ and so $x(t_1^+) = D^\mu$. Hence at the time of impulse the orbit is transported onto the critical orbit at $(D^\mu, \bar{s}^+)$. Thus, there are no more impulses and the orbit converges to the equilibrium point $(0, \mu)$. If the orbit starts in the region to the left and below this dotted curve, but to the right of the dash-dotted curve, then $\bar{s}$ is reached, and at the time of impulse the orbit is transported to the region to the left of the stable manifold of the equilibrium point $(0, \mu)$ above the line $s = \mu$ and converges to an equilibrium of the form $(0, s^*)$ with $s^* > \mu$, and so there are no more impulses. If (A_3) is satisfied the orbit starts in the region to the right or above this dotted curve.

If we are in the case i) depicted in Figure 3 (TOP), and start with initial conditions in the region to the right of the stable manifold of $(0, \mu)$ and above and to the right the dotted curve, then it can be shown that the process cycles indefinitely. All possible outcomes are summarized in the following Theorem.

Theorem 2.3. *Consider model (1) with $\bar{s} < \mu < \bar{s}^+$.*

1. *Assume that $\frac{1-r}{r} D_{\bar{s}} > D^\mu$. Then there exists a unique asymptotically stable periodic orbit with finite period $T > 0$. (See Figure 3 (TOP).)*
   - *i) An orbit with initial conditions satisfying (A_3) when $s(0) \leqslant \mu$, or (A_2) when $s(0) > \mu$, has an infinite sequence of impulse times $\{t_n\}_{n=1}^{\infty}$ and the orbit converges to the asymptotically stable periodic orbit.*

ii) For an orbit with initial conditions violating (A_3) *when* $s(0) \leqslant \mu$, *but satisfying* (A_1), *there exists a single* t_1 *such that* $s(t_1^-) = \bar{s}$, *and then* $s(t) > \mu$ *for all finite* $t > t_1$, *with* $s(t) \to s^* \geqslant \mu$ *as* $t \to \infty$ *and* $x(t) \to 0$ *as* $t \to \infty$.

iii) If $s(0) \leqslant \mu$ *and* (A_1) *is violated, then* $s(t) > \bar{s}$ *for all finite* $t > 0$ *and* $s(t) \to s^*$, *where* $\bar{s} \leqslant s^* < \lambda$, *as* $t \to \infty$ *and* $x(t) \to 0$ *as* $t \to \infty$. *If* $s(0) > \mu$ *and* (A_2) *is violated, then* $s(t) > \mu$ *for all finite* $t > 0$ *with* $s(t) \to s^* \geqslant \mu$ *as* $t \to \infty$ *and* $x(t) \to 0$ *as* $t \to \infty$.

In case i), the fermentor cycles indefinitely, and so there exists an infinite sequence of impulse times $\{t_n\}_{n=1}^{\infty}$. *As* $n \to \infty$, $t_n \to \infty$, $t_n - t_{n-1} \to T$, $x(t_n^-) \to \frac{1}{r} D_{\bar{s}}$ *and* $x(t_n^+) \to \frac{1-r}{r} D_{\bar{s}}$. *For all positive integers* n, *solutions satisfy* $s(t_n^+) = \bar{s}^+$ *and* $s(t_n^-) = \bar{s}$, *and either,*

a) $x(t_n^-) = \frac{1}{r} D_{\bar{s}}$, $x(t_n^+) = \frac{1-r}{r} D_{\bar{s}}$, *and* $t_{n+1} - t_n = T$, *hold for all* n,

b) $x(t_n^-) < \frac{1}{r} D_{\bar{s}}$, $x(t_n^+) < \frac{1-r}{r} D_{\bar{s}}$, $x(t_n^-) < x(t_{n+1}^-)$, $x(t_n^+) < x(t_{n+1}^+)$, *and* $t_n - t_{n-1} > t_{n+1} - t_n > T$, *hold for all* n, *or*

c) $x(t_n^-) > \frac{1}{r} D_{\bar{s}}$ $x(t_n^+) > \frac{1-r}{r} D_{\bar{s}}$, $x(t_n^-) > x(t_{n+1}^-)$, $x(t_n^+) > x(t_{n+1}^+)$, *and* $t_n - t_{n-1} < t_{n+1} - t_n < T$, *hold for all* n.

2. *Assume that* $\frac{1-r}{r} D_{\bar{s}} = D^{\mu}$. *There are no periodic orbits and for all orbits,* $\liminf_{t \to \infty} x(t) = 0$. *(See Figure 3 (MIDDLE).)*

i) An orbit with initial conditions satisfying (A_3) *when* $s(0) \leqslant \mu$, *or* (A_2) *when* $s(0) > \mu$, *converges to the critical curve. There are an infinite number of impulses, but the time between impulses increases monotonically and approaches infinity.*

ii) For an orbit with initial conditions violating (A_3) *when* $s(0) \leqslant \mu$, *but satisfying* (A_1), *there exists a single* t_1 *such that* $s(t_1^-) = \bar{s}$, *and then* $s(t) > \mu$ *for all finite* $t > t_1$, *with* $s(t) \to s^* \geqslant \mu$ *as* $t \to \infty$ *and* $x(t) \to 0$ *as* $t \to \infty$.

iii) If $s(0) \leqslant \mu$ *and* (A_1) *is violated, then* $s(t) > \bar{s}$ *for all finite* $t > 0$ *and* $s(t) \to s^*$, *where* $\bar{s} \leqslant s^* < \lambda$, *as* $t \to \infty$ *and* $x(t) \to 0$ *as* $t \to \infty$. *If* $s(0) > \mu$ *and* (A_2) *is violated, then* $s(t) > \mu$ *for all finite* $t > 0$ *with* $s(t) \to s^* \geqslant \mu$ *as* $t \to \infty$ *and* $x(t) \to 0$ *as* $t \to \infty$.

3. *Assume that* $\frac{1-r}{r} D_{\bar{s}} < D^{\mu}$. *There are at most a finite number of impulses. The time between impulses increases. Also* $s(t) > \bar{s}$ *for* t *sufficiently large, with* $s(t) \to s^* \geqslant \bar{s}$ *and* $x(t) \to 0$ *as* $t \to \infty$. *(See Figure 3 (BOTTOM).)*

In all cases except case *1. i)*, Theorem 2.3 predicts that the process fails. In case *1,* success depends on the choice of initial conditions. If the process undergoes two impulses, then it will cycle indefinitely with a bounded time between impulses. In case *2,* $\frac{1-r}{r} D_{\bar{s}} = D^{\mu}$, solutions that undergo two impulses, also undergo an infinite number of impulses, but the time between impulses increases without bound and the population of microorganisms essentially washes out. In case *3,* $0 < \frac{1-r}{r} D_{\bar{s}} < D^{\mu}$, solutions undergo at most a finite number of impulses, and eventually the microorganisms wash out.

Theorem 2.4. *Consider model (1) with* $\mu \leqslant \bar{s} < \bar{s}^+$. *In this case,* $\frac{1-r}{r} D_{\bar{s}} < D^{\mu}$. *System (1) admits no periodic orbit. If initial conditions satisfy* (A_1), *then there are at most a finite number of impulses. If initial conditions violate* (A_1), *then there are no impulses. In both cases,* $s(t) \to s^* \geqslant \bar{s}$ *and* $x(t) \to 0$ *as* $t \to \infty$.

The cases $\bar{s} < \mu < \bar{s}^+$ and $\mu \leqslant \bar{s} < \bar{s}^+$ were considered in Theorems 2.3 and 2.4, respectively. It remains to consider the case, $\bar{s} < \bar{s}^+ \leqslant \mu$. If $s(0) \leqslant \mu$, this

was resolved in [23]. The outcome depends on the sign of $D_{\bar{s}}$ (called s_{int} in [23]). If $D_{\bar{s}} > 0$, the process is successful for appropriate initial conditions, otherwise it fails. If $s(0) > \mu$, and (A_2) holds, after the first impulse, $s(t_1^+) \leqslant \mu$ and we are back in the case just discussed. However, if $s(0) > \mu$ and (A_2) is violated, then the process fails. There are no impulses and $x(t) \to 0$ and $s(t) \to s^* \geqslant \mu$ as $t \to \infty$.

3. **Simulations.** In 1930, Haldane [14] derived the following form to model the activity of a substrate-inhibited enzyme,

$$f(s) = \frac{ms}{(k_s + s)(1 + \frac{s}{k_i})}. \tag{8}$$

Here s denotes the concentration of the substrate; m the maximum specific growth rate; k_s the half-saturation coefficient; and k_i the inhibition coefficient.

Andrews [4], popularized the mathematically similar form,

$$f(s) = \frac{ms}{k_s + s + \frac{s^2}{k_i}}. \tag{9}$$

to model the specific growth rate of microorganisms inhibited at high as well as low concentrations of substrate.

Many different forms for the response function have been proposed and tested. See for example Aiba et. al [1], Alagappan and Cowan [2, 3], Boon and Landelout [8], Edwards [12], Luong [16], and Wayman and Tseng [25].

In particular, Wayman and Tseng [25] modified the Monod form

$$WT(s) = \begin{cases} \frac{ms}{k_s+s} & \text{if } s < s_0, \\ \frac{ms}{k_s+s} + i(s - s_0) & \text{if } s \geq s_0, \end{cases} \tag{10}$$

where the parameters m and k_s have the same interpretation as before, i is an inhibition coefficient, and s_0 is the threshold of the substrate concentration below which there is no apparent inhibition.

Recently, Alagappan and Cowan [2] proposed the following modification of the Wayman and Tseng form,

$$mWT(s) = \begin{cases} \frac{ms}{k_s+s+\frac{s^2}{k_i}} & \text{if } s < s_0, \\ \frac{ms}{k_s+s+\frac{s^2}{k_i}} + i(s - s_0) & \text{if } s \geq s_0, \end{cases} \tag{11}$$

and in [3] tested this form against the forms of Andrews, Luong, Wayman and Tseng, and Aiba et. al. for the growth of several different microorganisms on benzene or toluene. They found that in the case of biodegradation of toluene, for Pseudomonas Putipda F1 and mt2, the Wayman-Tseng model (10) provided the best fit to their data, whereas for Ralstonia picketti PKO1 the modified Wayman-Tseng model (11) provided the best fit. See Table 1 for the response functions and species specific parameters that they found best fitted their data and Figure 4 for the corresponding graphs of these response functions of best fit.

By means of numerical simulations using MATLAB we show an example for which the model predicts successful implementation of the self-cycling fermentation process in the case of biodegradation of toluene by Ralstonia picketti PKO1.

This example illustrates Theorem 2.3.*1. i).* Here, $\bar{s} < \lambda < \mu < \bar{s}^+$ and $(1 - r)D_{\bar{s}} > rD^{\mu}$. In most applications, $s(0) = s^i > \bar{s}^+ > \mu$, and so, in this case, as long as (A_2) is satisfied, i.e. the process starts with enough microorganisms in the tank, the model predicts that the fermentor will cycle indefinitely, approaching the state described by the unique orbitally asymptotically stable periodic orbit

TABLE 1. Response functions and corresponding parameters of best fit from [3] for biodegradation of toluene.

Strain	1	2	3	4
Name	Ralstonia pickettii PKO1	Pseudomonas putida mt2	Pseudomonas putida F1	Hypothetical species
$f(s)$	$mWT(s)$	$WT(s)$	$WT(s)$	$mWT(s)$

	Species Specific Parameters					
	m (h^{-1})	k_s (mg/L)	k_i (mg/L)	s_0 (mg/L)	i (L mg h)	S_{max} (mg/L)
1	0.48	3.20	352	220	0.002	341
2	0.36	0.97	–	206	0.0019	395
3	0.35	0.58	–	278	0.0028	402
4	0.37	0.24	339	163	0.00085	370

	$\bar{d}$ (h^{-1})	λ (mg/L)	μ (mg/L)	Y (mg/L)
1	0.11	0.95	294	1.05
2	0.065	0.21	360	1.25
3	0.06	0.12	381	1.34
4	0.041	0.02	333	1.43

with a bounded cycle time (see the two orbits in phase space in Figure 5 and the corresponding time series in Figure 6). From the time series, one can see that the cycle time of the orbit approaching from the left increases and the cycle time of the orbit approaching from the right decreases to the cycle time of the attracting periodic orbit, as predicted by Theorem 2.3.*1. i) b) - c).*

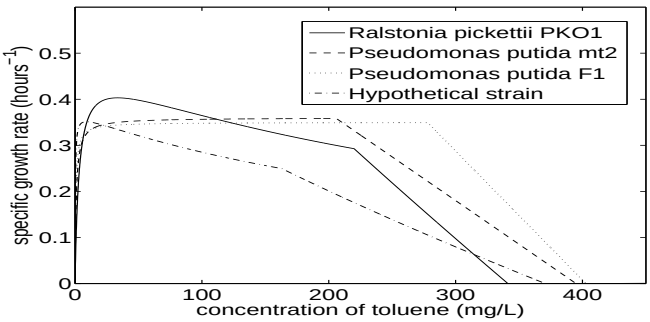

FIGURE 4. The response functions for Pseudomonas putida mt2 and F1 are modelled using the Wayman-Tseng form (10) and for Ralstonia pickettii PKO1 and the "Hypothetical strain" by the modified Wayman-Tseng form (11). See Table 1 for the parameter values.

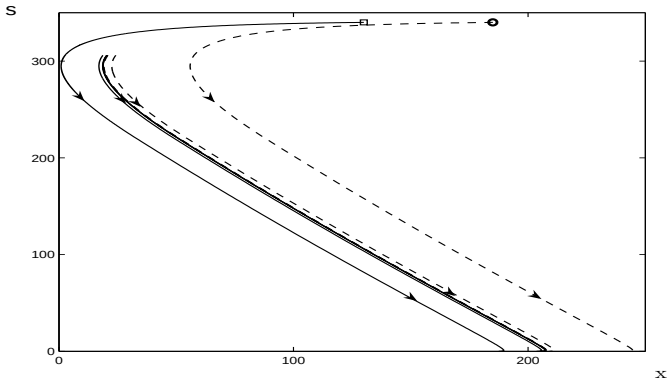

FIGURE 5. Graph of two orbits in phase space that cycle indefinitely and show successful operation of the fermentor in the case of biodegradation of toluene by Strain 1, Ralstonia picketti PKO1. See Table 1 for the response function and species specific parameters used. Other operating parameters were chosen to be: $s^i = 340$ mg/L, $\bar{s} = 0.024$ mg/L, $r = 0.9$, and so $\bar{s}^+ = 306$ mg/L, $\lambda = 0.95$ mg/L, $\mu = 294$ mg/L, $D_{\bar{s}} = 184.9$, and $D^\mu = 1.70$. Therefore, $\bar{s} < \lambda < \mu < \bar{s}^+$ and $(1-r)D_{\bar{s}}(r) = 18.49 > 1.53 = rD^\mu(r)$. The two orbits, one (dashed) approaches the orbitally asymptotically stable periodic orbit, from the right, and the other (solid) approaches it from the left. At each impulse, there is a discontinuity. The dashed orbit moves further to the left and the solid orbit moves further to the right. Both orbits become almost indistinguishable from the periodic orbit in approximately $3-4$ cycles. Initial conditions of the solid orbit are $x(0) = 130$, $s(0) = s^i$ and of the dashed orbit are $x(0) = 185$, $s(0) = s^i$.

4. **The emptying and refilling fraction.** In their experiments, Wincure, Cooper, and Rey [27] chose the emptying and refilling fraction to be $r = \frac{1}{2}$. However, in [23] it was shown that the fraction that maximizes the efficiency need not be $\frac{1}{2}$ and described how to find the *best* r.

Before considering how to find the *best* r, we consider whether values of the emptying and refilling fraction can be found for which the process can be successful, if appropriate initial conditions are chosen (see Theorem 2.3.*1. i)*), once all parameters except r are determined.

In the following Theorem we indicate that if the fermentor can be operated successfully for one choice of $r \in (0,1)$, then there is an open interval, $(r_0, r^0) \subset [0,1]$, containing all possible choices of r that will result in successful operation. By Theorem 2.4, if $\bar{s} \geqslant \mu$, the process cannot succeed. Hence, we assume that $\bar{s} < \mu$, throughout this section. We think of $D_{\bar{s}}$ and D^μ as functions of r, and denote them by $D_{\bar{s}}(r)$ and $D^\mu(r)$.

We are particularly interested in where the functions $(1-r)D_{\bar{s}}(r)$ and $rD_\mu(r)$ intersect. See Figure 7 for an example of biodegradation of toluene by Ralstonia pickettii PKO1, based on the response function form and parameters shown to be the best fit in [3] (see Tables 1 and 2).

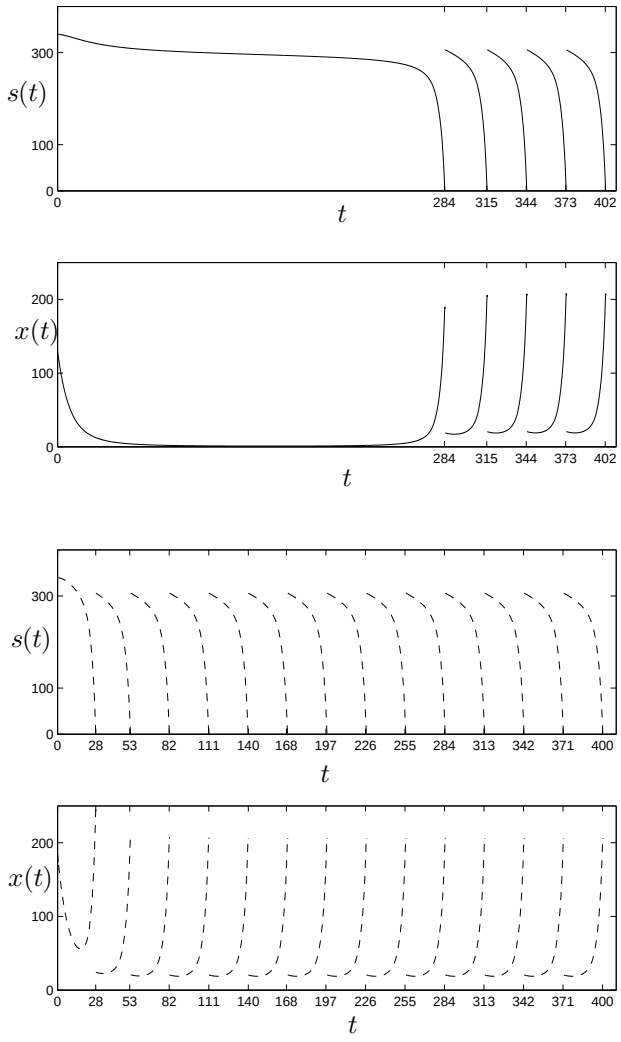

FIGURE 6. The corresponding time series, of the orbits depicted in Figure 5. The cycle time of the solid orbit (the one that approaches from the left in the phase portrait) decreases and the cycle time of the dashed orbit (the one approaching from the right) increases approaching the period of the attracting periodic orbit, approximately 29 hours.

Theorem 4.1. *Fix all parameters except r. Assume that $\bar{s} < \mu$. Define* $r^* = \min(1, \frac{\mu - \bar{s}}{s^i - \bar{s}})$.

1. *If $(1-r^*)D_{\bar{s}}(r^*) > r^* D^{\mu}(r^*)$, then there exists a nonempty interval $(r_0, r^0) \subset [0,1]$ such that $(1-r)D_{\bar{s}}(r) > rD^{\mu}(r)$ for all $r \in (r_0, r^0)$, and for any r in this interval, initial conditions exist for which the process cycles indefinitely with finite cycle time, and hence is successful. If $r \notin (r_0, r^0)$, the process fails.*
   (a) If $\bar{s} < \lambda$, then $r_0 > 0$. If $\bar{s} \geqslant \lambda$, then $r_0 = 0$.
   (b) If $\mu < s^i$, then $r^0 < 1$. If $\mu \geqslant s^i$, then $r^0 = 1$.

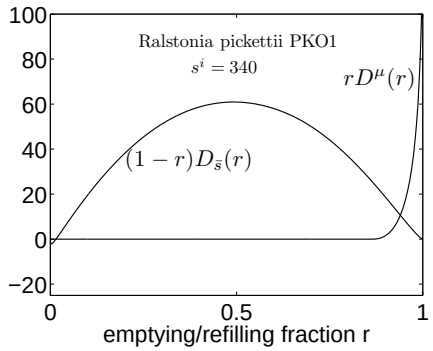

FIGURE 7. The graphs of $(1-r)D_{\bar{s}}(r)$ and $rD^\mu(r)$ as r varies, for Ralstonia pickettii limited by toluene with $s^i = 340$ and $\bar{s} = .024$. See Table 1 for the response function and parameter values used. In this case, $\lambda = 0.95$ mg/L and $\mu = 294$ mg/L and so $\bar{s} < \lambda < \mu < s^i$, and so $r_0 = 0.015 > 0$ and $r^0 = 0.93 < 1$.

2. *If* $(1-r^*)D_{\bar{s}}(r^*) \leqslant r^* D^\mu(r^*)$, *then* $(1-r)D_{\bar{s}}(r) \leqslant rD^\mu(r)$ *for all* $r \in (0,1)$, *and the process fails for any choice of* r.

From Theorem 4.1 it follows immediately that if a population of microorganisms can be chosen so that $\lambda < \bar{s} \leqslant s^i \leqslant \mu$, then any choice of $r \in (0,1)$ would theoretically result in success for some choice of initial conditions. See Table 2 for the values of r_0, r^0 and r^*, for the strains considered in Table 1.

Now we consider how to choose r in order to maximize the yield, and hence the efficiency, of the self-cycling fermentation process. By the yield, we mean the total volume of medium processed over some fixed time period, $\mathcal{T}$, where $\mathcal{T}$ is relatively long compared to the time between impulses.

For successful operation, besides requiring that $\frac{(1-r)}{r}D_{\bar{s}}(r) > D^\mu(r)$, initial conditions must be selected appropriately. If so, after a finite number of impulses, orbits are almost indistinguishable from the attracting cycle. Thus, for the purpose of comparing yields, for different values of r, just as in [23], since we are assuming $\mathcal{T}$ is large compared to the cycle time, we choose initial conditions on the periodic orbit, that is, $x(0) = \frac{1-r}{r}D_{\bar{s}}$ and $s(0) = \bar{s}^+$.

We represent the yield by

$$\Omega(r) \quad = \quad \frac{rV}{T(r) + (\alpha(V)r + \epsilon)}\mathcal{T}. \tag{12}$$

where r is the emptying/refilling fraction, assumed to be strictly between r_0 and r^0, V is the volume of medium in the tank, which is assumed to be constant except during the emptying and refilling time, $T(r)$ is the period of the periodic orbit and hence the time between impulses, $\alpha(V)r + \epsilon$ is the time taken to empty and refill the tank, and $\mathcal{T} \gg T(r)$ is the fixed period of time over which the total yield is calculated. Our goal is to

$$\text{find} \quad \bar{r} \in (r_0, r^0), \quad \text{such that} \quad \Omega(\bar{r}) = \max_{r \in (r_0, r^0)} \Omega(r).$$

The expression for the yield given in (12) is more realistic than the expression given in [23], where the term in brackets was instead approximated by a constant, and so was independent of r. Here we take into consideration that the larger the fraction

TABLE 2. Comparing effectivenesss of strains for different levels of the pollutant, toluene.

Simulation	$\bar{s}$ (mg/L)	$\alpha(V)$ (hour)	ϵ (hour)	$\mathcal{T}$ (hour)
Parameters	0.024	1/60	4.5/60	100000

Strains	Initial level of pollutant toluene, s^i=100 mg/L						
	r_0	r^0	r^*	$\bar{r}$	$\bar{s}^+_{\bar{r}}$ (mg/L)	$T(\bar{r})$ (hour)	$\Omega(\bar{r})$ (litres)
1	0.05	1	1	0.47	47.40	3.46	13350
2	0.007	1	1	0.33	33.03	1.76	17854
3	0.003	1	1	0.28	28.14	1.36	19459
4	0.0001	1	1	0.20	20.67	0.79	23607

Strains	Initial level of pollutant toluene, s^i=250 mg/L						
	r_0	r^0	r^*	$\bar{r}$	$\bar{s}^+_{\bar{r}}$ (mg/L)	$T(\bar{r})$ (hour)	$\Omega(\bar{r})$ (litres)
1	0.02	1	1	0.30	76.54	1.90	15430
2	0.0029	1	1	0.26	65.11	1.24	19663
3	0.0012	1	1	0.23	57.85	1.03	20833
4	0.00005	1	1	0.16	40.46	0.60	23539

Strains	Initial level of pollutant toluene, s^i=340 mg/L						
	r_0	r^0	r^*	$\bar{r}$	$\bar{s}^+_{\bar{r}}$ (mg/L)	$T(\bar{r})$ (hour)	$\Omega(\bar{r})$ (litres)
1	0.015	0.93	0.865	0.25	87.64	1.55	15810
2	0.0021	1	1	0.24	82.97	1.13	20083
3	0.00093	1	1	0.22	74.90	0.96	21135
4	0.000037	0.99	0.979	0.14	50.22	0.55	23274

of the tank emptied, the longer it takes. See Table 2 for the values of $\bar{s}, \alpha(V), \epsilon$ and $\mathcal{T}$ used in all of the simulations in this section. For the purpose of comparison, the volume V was assumed to be one liter. Selection of a more appropriate tank size would likely be more efficient in practice.

The following explicit formula for $T(r)$ was derived in [23],

$$T(r) = \int_{\bar{s}}^{\bar{s}^+} \frac{Y}{f(s)} \left(\frac{1}{\frac{(1-r)}{r} D_{\bar{s}} + Y \int_s^{\bar{s}^+} \left(1 - \frac{\bar{d}}{f(u)}\right) du} \right) ds. \tag{13}$$

We compare the cycle time and the yield for a hypothetical strain and three of the five pure cultures of toluene degrading strains, Ralstonia pickettii PKO1, Pseudomonas putida F1, and Pseudomonas putida mt2, considered in Table V of [3], where they provide the best functional form to model the specific growth rates along with the parameters giving the best fit. This information is summarized in Table 1 and Figure 8. We did not consider two of the strains considered in [3], since the specific growth rates of those strains were lower than that of Pseudomonas putida mt2 for all concentrations of toluene considered, and so clearly they would

not be as efficient. The hypothetical strain was found by accident, i.e. parameters for one of the omitted strains was entered incorrectly. However, we include the results for this strain, since the parameters are reasonable and we found the result surprising and informative with respect to how to choose the most effective strain.

The hypothetical strain was the most effective over a large range of the input contaminant levels s^i, even though its specific growth rate is lower than that of the other populations over a wide range of concentrations of the contaminant. It seems that, having a high specific growth rate at very low levels of the contaminant is more important than having a high specific growth rate at moderate to high levels. This observation is also consistent with the second most effective strain, Pseudomonas putida F1. Compare the specific growth rates in Figure 4 and the yields in Figure 8 for input pollutant levels $s^i = 100$ and 250 mg/L.

Note also that the theoretical optimal yield may require $\bar{r}$ to be too close to zero or too close to 1 to be implementable. Figure 8 shows that although one strain might have the optimal yield for a particular value of r, it need not be the most effective for all values of r. Thus, if the optimal value $\bar{r}$ is not implementable, further investigation is necessary. See in particular Figure 8 in the case that $s^i = 340$ mg/L, where the optimal value of r is quite small for the most effective strain, the hypothetical strain. If for example it is not practical to choose $r < 0.4$, it might be advantageous to operate the fermentor with a different strain, the Pseudomonas putida F1, in this case. In any case, understanding how to choose the best emptying/refilling fraction for the particular situation can help to improve the effectiveness of the process.

5. **Proofs.**

Throughout this section we assume that $\bar{d} > 0$ unless otherwise specified. Before proving the Theorems we give a number of Lemmas.

Lemma 5.1. *Let $\tilde{\gamma}(t)$ and $\hat{\gamma}(t)$ be two orbits of (3), with the initial conditions, $(\tilde{x}(0), \tilde{s}(0))$ and $(\hat{x}(0), \hat{s}(0))$, respectively, satisfying $\tilde{s}(0) = \hat{s}(0)$, but $\tilde{x}(0) - \hat{x}(0) = \eta > 0$. For any times $\tilde{t} > 0$ and $\hat{t} > 0$, where $\tilde{s}(\tilde{t}) = \hat{s}(\hat{t})$, it follows that $\tilde{x}(\tilde{t}) - \hat{x}(\hat{t}) = \eta$ and $\tilde{t} < \hat{t}$.*

Proof. See Lemma 1 of [23]. □

Lemma 5.2. *Let $\gamma(t) = (x(t), s(t))$ be an orbit of (3) with $x(0) > 0, s(0) > \bar{s}$. If either*

i) $s(0) > \bar{s} \geqslant \mu$ and (A_1) holds,
ii) $\mu \geqslant s(0) > \bar{s}$ and (A_1) holds, or
iii) $s(0) > \mu > \bar{s}$ and (A_1) and (A_2) hold,

then there exists $t_1 > 0$, finite, such that $x(t_1) > 0$ and $s(t_1) = \bar{s}$.

Proof. It is clear that the vector field for system (3) is C^1. From the phase portrait (see Figure 1 (RIGHT)), all orbits are bounded, there are no equilibria with both components positive, and $s(t)$ is strictly decreasing. The s-axis consists entirely of equilibria and for all orbits with $x(0) > 0$ initiating on the x-axis, $s(t) \equiv 0$ and $x(t) \to 0$ as $t \to \infty$. Therefore, for all orbits with positive initial conditions, $x(t) \to 0$ and $s(t) \to s^* > 0$ as $t \to \infty$.

First, assume that case *iii)* holds. We begin by proving that there exists a $\hat{t} > 0$, finite, so that $s(\hat{t}) = \mu$ and $x(\hat{t}) > 0$. Suppose not, i.e., assume that $s(t) \to s^* \geqslant \mu$

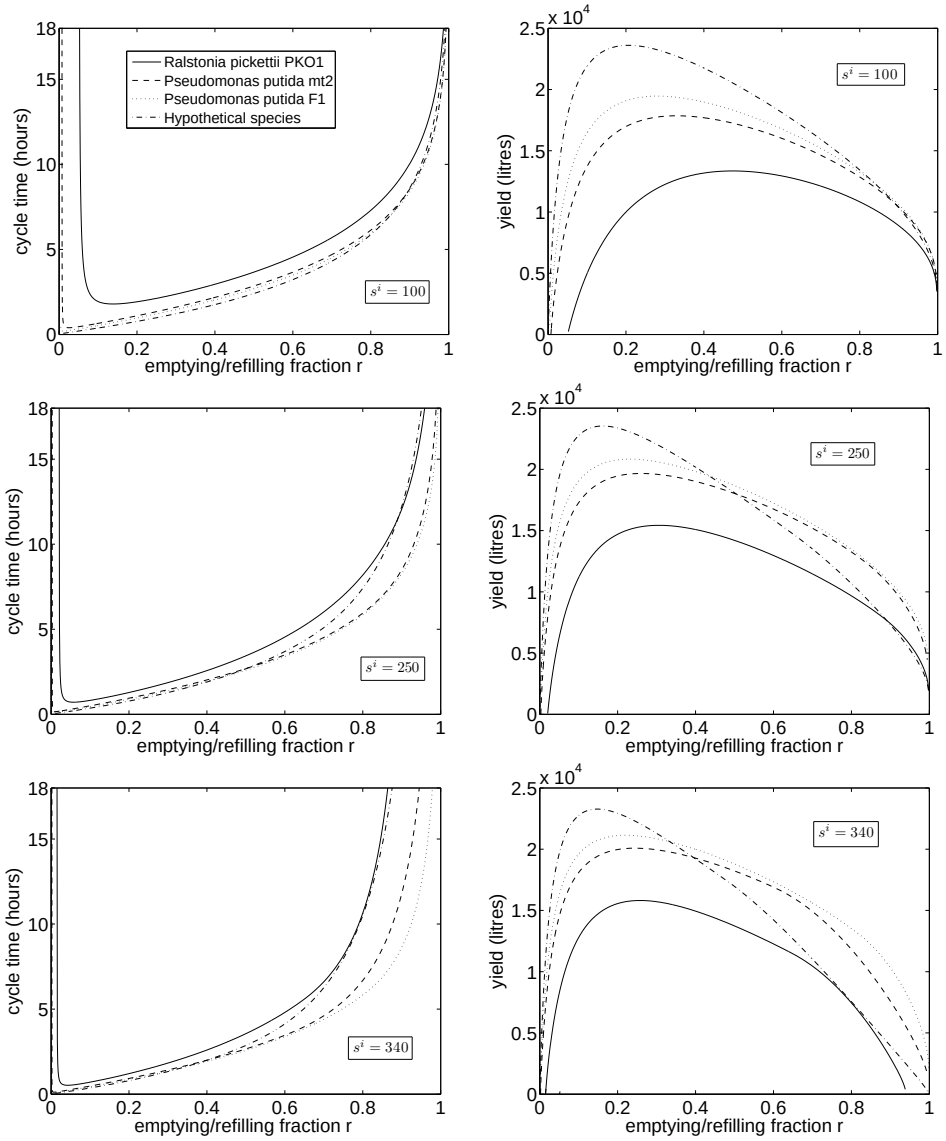

FIGURE 8. (LEFT) Cycle time (period of the attracting periodic orbit) and (RIGHT) yield as r varies, for the biodegradation of toluene by several strains for different levels of contamination by toluene. Tables 1 and 2 give the response functions, parameter values, and results of the simulations, including the optimal emptying/refilling fraction and corresponding cycle time and yield. For all three levels of the contaminant, the optimal yield was obtained by the hypothetical strain, followed by Pseudomonas putida F1, Pseudomonas putida mt2, and Ralstonia pickettii PKO1. However, for larger (nonoptimal) values of the emptying/refilling fraction, Pseudomonas putida F1 was most effective. It is not the strain that has the highest specific growth rate over the largest range of toluene concentration (see Figure 4), but rather the one that has the highest specific growth rate over very low concentrations of toluene, just above the threshold $\bar{s}$, that appears to be most efficient.

as $t \to \infty$. Then, since $x(t) \to 0$ as $t \to \infty$, by (5)

$$\begin{aligned} 0 &= \lim_{t\to\infty} x(t) = x(0) + Y\int_{s^*}^{s(0)} \left(1 - \frac{\bar{d}}{f(s)}\right) ds \\ &\geqslant x(0) + Y\int_{s^*}^{s(0)} \left(1 - \frac{\bar{d}}{f(s)}\right) ds + Y\int_{\mu}^{s^*} \left(1 - \frac{\bar{d}}{f(s)}\right) ds \\ &= x(0) + Y\int_{\mu}^{s(0)} \left(1 - \frac{\bar{d}}{f(s)}\right) ds \\ &> 0, \qquad \text{by } (A_2). \end{aligned}$$

From this contradiction we conclude that $s^* < \mu$. It follows immediately from the vector field (see Figure 1 (RIGHT)), that $s^* < \lambda$. Suppose $s^* \geqslant \bar{s}$. Since

$$\begin{aligned} 0 &= \lim_{t\to\infty} x(t) = x(0) + Y\int_{s^*}^{s(0)} \left(1 - \frac{\bar{d}}{f(s)}\right) ds \\ &\geqslant x(0) + Y\int_{s^*}^{s(0)} \left(1 - \frac{\bar{d}}{f(s)}\right) ds + Y\int_{\bar{s}}^{s^*} \left(1 - \frac{\bar{d}}{f(s)}\right) ds \\ &= x(0) + Y\int_{\bar{s}}^{s(0)} \left(1 - \frac{\bar{d}}{f(s)}\right) ds \\ &> 0, \qquad \text{by } (A_1), \end{aligned}$$

a contradiction. Therefore, $s^* < \bar{s}$ and so there exists a finite $t_1 > 0$ such that $s(t_1) = \bar{s}$. The proofs of cases (i) and (ii) are similar. □

Lemma 5.3. *Let $\gamma(t) = (x(t), s(t))$ be an orbit of (3) with $x(0) > 0, s(0) > \bar{s}$. If (A_1) is not satisfied, then $s(t) > \bar{s}$ and for all finite t, $s(t) \to s^* \geqslant \bar{s}$ and $x(t) \to 0$ as $t \to \infty$.*

Proof. Assume that (A_1) is not satisfied. We proceed using proof by contradiction. Suppose there exists at least one finite $\tilde{t}$ such that $s(\tilde{t}) = \bar{s}$. By (5),

$$x(\tilde{t}) = x(0) + Y\int_{s(\tilde{t})}^{s(0)} \left(1 - \frac{\bar{d}}{f(s)}\right) ds = x(0) + Y\int_{\bar{s}}^{s(0)} \left(1 - \frac{\bar{d}}{f(s)}\right) ds \leqslant 0,$$

since (A_1) is not satisfied. This is impossible, since the s-axis is made up of equilibria that can not be reached or crossed in finite time. Therefore, $s(t) > \bar{s}$ for all finite t. The result follows immediately (see Figure 1 (RIGHT)) □

Lemma 5.4. *Let $\gamma(t) = (x(t), s(t))$ be an orbit of (3) with $x(0) > 0, s(0) > \bar{s}$. Assume $\bar{s} < \mu < s(0)$.*

i) If (A_2) is not satisfied, then $s(t) > \mu$ for all finite t, and $s(t) \to s^* \geqslant \mu$ as $t \to \infty$.

ii) If (A_2) is satisfied, but (A_1) is not satisfied, then $s(t) > \bar{s}$ for all finite t and $s(t) \to s^* \geqslant \bar{s}$ as $t \to \infty$, where $\bar{s} \leqslant s^* < \lambda$.

Proof. Suppose that $\bar{s} < \mu < s(0)$. *i)* First, assume that (A_2) is not satisfied. If there exists a finite $\tilde{t}$ such that $s(\tilde{t}) = \mu$, by (5),

$$x(\tilde{t}) = x(0) + Y\int_{s(\tilde{t})}^{s(0)} \left(1 - \frac{\bar{d}}{f(s)}\right) ds = x(0) + Y\int_{\mu}^{s(0)} \left(1 - \frac{\bar{d}}{f(s)}\right) ds \leqslant 0,$$

since (A_2) is not satisfied. This is impossible, since the s-axis is made up of equilibria that cannot be reached within finite time. Therefore, $s(t) > \mu$ for all finite

t. The result now follows directly from the properties of the vector field (see Figure 1 (RIGHT)).

ii) Assume (A_2) is satisfied, but not (A_1). As in the proof of Lemma 5.2, there exists a $\hat{t} > 0$, finite, such that $s(\hat{t}) = \mu$ and $x(\hat{t}) > 0$. Recall that $s(t)$ is strictly decreasing. From the phase portrait it now follows that $s(t) > \mu$ for $t < \hat{t}$ and $s(t) < \mu$ for $t > \hat{t}$. Since (A_1) is not satisfied, the result follows immediately from Lemma 5.3. □

The following two Lemmas concern system (1).

Lemma 5.5. *Let $\gamma(t) = (x(t), s(t))$ be an orbit of (1). Assume that $\bar{s}^+ > \mu$, $\frac{1-r}{r} D_{\bar{s}} \geqslant D^\mu$, and there exists a finite t_1 such that $s(t_1^-) = \bar{s}$. Then if (A_3) holds, there is an increasing sequence of distinct times $\{t_n\}_{n=1}^{\infty}$, such that $s(t_n^-) = \bar{s}, s(t_n^+) = \bar{s}^+$, and $x(t_n^+) > D^\mu$; if (A_3) is violated, the only impulse occurs at $t = t_1$ and $s(t) > \mu$ for all finite $t > t_1$, $s(t) \to s^* \geqslant \mu$, $x(t) \to 0$ as $t \to \infty$.*

Proof. Since $s(t_1^-) = \bar{s}$ for t_1 finite, it follows that $x(t_1^-) > 0$. The s-axis is composed of equilibria and so $x(t)$ cannot reach 0 within finite time. By (5),

$$x(t_1^-) = x(0) + Y \int_{s(t_1^-)}^{s(0)} \left(1 - \frac{\bar{d}}{f(s)}\right) ds = x(0) + Y \int_{\bar{s}}^{s(0)} \left(1 - \frac{\bar{d}}{f(s)}\right) ds.$$

First, suppose (A_3) holds. From the impulse condition of (1),

$$\begin{aligned} s(t_1^+) &= s(t_1^-) - r\bar{s} + rs^i = (1-r)\bar{s} + rs^i = \bar{s}^+, \\ x(t_1^+) &= x(t_1^-) - rx(t_1^-) \\ &= (1-r)x(t_1^-) \\ &= (1-r)\left(x(0) + Y \int_{\bar{s}}^{s(0)} \left(1 - \frac{\bar{d}}{f(s)}\right) ds\right) \\ &> D^\mu, \qquad \text{by } (A_3). \end{aligned} \tag{14}$$

At time t_1, (x, s) instantly jumps from point $(x(t_1^-), \bar{s})$ to $(x(t_1^+), \bar{s}^+)$ and continues to move along the curve $(x(t), s(t))$ described by the solution of system (3) with the new initial condition $(x(t_1^+), s(t_1^+))$, where $s(t_1^+) = \bar{s}^+$. Since $\bar{s}^+ > \mu$, it follows that $s(t_1^+) = \bar{s}^+ > \mu$. Since $f(s) < \bar{d}$ for $\mu < s < \bar{s}^+$,

$$D^\mu \equiv Y \int_{\mu}^{\bar{s}^+} \left(\frac{\bar{d}}{f(s)} - 1\right) ds > 0.$$

Since $\frac{1-r}{r} D_{\bar{s}} \geqslant D^\mu$ and $D^\mu > 0$, we obtain $D_{\bar{s}} > 0$. By (14),

$$x(t_1^+) > D^\mu = Y \int_{\mu}^{\bar{s}^+} \left(\frac{\bar{d}}{f(s)} - 1\right) ds,$$

and so

$$x(t_1^+) + Y \int_{\mu}^{\bar{s}^+} \left(1 - \frac{\bar{d}}{f(s)}\right) ds > 0.$$

In addition,

$$x(t_1^+) + Y \int_{\bar{s}}^{\bar{s}^+} \left(1 - \frac{\bar{d}}{f(s)}\right) ds = x(t_1^+) + D_{\bar{s}} > 0.$$

Therefore, the new initial condition $(x(0), s(0)) = (x(t_1^+), s(t_1^+))$ in system (3) satisfies (A_2) and (A_1). The hypotheses of case *iii)* in Lemma 5.2 are satisfied. Therefore, there exists $t_2 > t_1$ such that $s(t_2^-) = \bar{s}$. Again from (5), we obtain

$$\begin{aligned} x(t_2^-) &= x(t_1^+) + Y \int_{s(t_2^-)}^{s(t_1^+)} \left(1 - \frac{\bar{d}}{f(s)}\right) ds \\ &= x(t_1^+) + Y \int_{\bar{s}}^{\bar{s}^+} \left(1 - \frac{\bar{d}}{f(s)}\right) ds \\ &= x(t_1^+) + D_{\bar{s}}. \end{aligned}$$

By the impulse condition of (1),

$$\begin{aligned} s(t_2^+) &= s(t_2^-) - r\bar{s} + rs^i = (1-r)\bar{s} + rs^i = \bar{s}^+ \\ x(t_2^+) &= (1-r)x(t_2^-) \\ &= (1-r)\left(x(t_1^+) + D_{\bar{s}}\right) \\ &> (1-r)D^\mu + (1-r)D_{\bar{s}} \\ &\geqslant (1-r)D^\mu + rD^\mu \\ &= D^\mu. \end{aligned}$$

Just as for t_1^+, we can show that (A_1) and (A_2) are satisfied for $(x(t_2^+), s(t_2^+))$. Again, case *iii)* in Lemma 5.2 holds. It follows that there is a time $t_3 > t_2$ such that $s(t_3^-) = \bar{s}$, $s(t_3^+) = \bar{s}^+$ and $x(t_3^+) > D^\mu$. This process can be repeated without end. Hence, there is an increasing sequence of distinct impulse times $\{t_n\}_{n=1}^\infty$ such that $s(t_n^-) = \bar{s}$, $s(t_n^+) = \bar{s}^+$, and $x(t_n^+) > D^\mu$.

If (A_3) is violated, then

$$x(t_1^+) \leqslant D^\mu \qquad \textit{and} \qquad s(t_1^+) = \bar{s}^+.$$

At time t_1, (x, s) instantly jumps from point $(x(t_1^-), \bar{s})$ to $(x(t_1^+), \bar{s}^+)$ and continues to move along the curve $(x(t), s(t))$ described by the solution of system (3) with new initial condition $(x(t_1^+), s(t_1^+))$. By Lemma (5.4)*i)* with initial condition equal to $(x(t_1^+), s(t_1^+))$, $s(t) > \mu$ for all finite $t > t_1$, $s(t) \to s^* \geqslant \mu$, and $x(t) \to 0$, as $t \to \infty$. □

Lemma 5.6. *Consider an orbit $(x(t), s(t))$ of (1). If there exists an increasing sequence of distinct times $\{t_n\}_{n=1}^\infty$ such that $s(t_n^-) = \bar{s}$, then*

$$x(t_n^-) = \frac{1}{r} D_{\bar{s}} + (1-r)^{n-1} \left(x(t_1^-) - \frac{1}{r} D_{\bar{s}}\right),$$

$$x(t_n^+) = \frac{1-r}{r} D_{\bar{s}} + (1-r)^n \left(x(t_1^-) - \frac{1}{r} D_{\bar{s}}\right),$$

and so $x(t_n^-) \to \frac{1}{r} D_{\bar{s}}$, $x(t_n^+) \to \frac{1-r}{r} D_{\bar{s}}$ as $n \to \infty$.

If $x(t_1^-) > \frac{1}{r} D_{\bar{s}}$, $\{x(t_n^-)\}$ and $\{x(t_n^+)\}$ are decreasing sequences, and if $x(t_1^-) < \frac{1}{r} D_{\bar{s}}$, $\{x(t_n^-)\}$ and $\{x(t_n^+)\}$ are increasing sequences. If $x(t_1^-) = \frac{1}{r} D_{\bar{s}}$, then $x(t_n^+) = \frac{1}{r} D_{\bar{s}}$, $x(t_n^-) = \frac{1-r}{r} D_{\bar{s}}$ for all positive integers n.

Proof. From (5),

$$x(t_n^-) = x(t_{n-1}^+) + D_{\bar{s}} = (1-r)x(t_{n-1}^-) + D_{\bar{s}}, \qquad n = 2, 3, 4, \cdots.$$

Solving these, we obtain

$$\begin{aligned} x(t_n^-) &= (1-r)^{(n-1)}x(t_1^-) + D_{\bar{s}}\left(1+(1-r)+\cdots+(1-r)^{(n-2)}\right) \\ &= (1-r)^{(n-1)}x(t_1^-) + D_{\bar{s}}\left(\frac{1-(1-r)^{(n-1)}}{r}\right) \\ &= \frac{1}{r}D_{\bar{s}} + (1-r)^{n-1}\left(x(t_1^-) - \frac{1}{r}D_{\bar{s}}\right), \qquad n = 2,3,4,\cdots. \end{aligned}$$

Therefore,

$$x(t_n^+) = (1-r)x(t_n^-) = \frac{1-r}{r}D_{\bar{s}} + (1-r)^n\left(x(t_1^-) - \frac{1}{r}D_{\bar{s}}\right),\ n = 2,3,4,\cdots,$$

and the limiting and monotonicity properties follow immediately. □

Lemma 5.7. *Consider system (1) with* $\frac{1-r}{r}D_{\bar{s}} \geqslant D^{\mu}$. *If* $s(0) > \mu$ *and* (A_2) *holds, then* (A_3) *holds.*

Proof. From $\frac{1-r}{r}D_{\bar{s}} \geqslant D^{\mu}$, we obtain

$$D^{\mu} + D_{\bar{s}} \geqslant D^{\mu} + \frac{r}{1-r}D^{\mu} \geqslant \frac{(1-r)D^{\mu} + rD^{\mu}}{1-r} \geqslant \frac{D^{\mu}}{1-r}.$$

If $s(0) > \mu$ and (A_2) is satisfied, as in the proof of Lemma 2, there exists $\hat{t} > 0$ such that $x(\hat{t}) > 0$ and $s(\hat{t}) = \mu$. We proceed by showing that there is a finite t_1 $(> \hat{t})$ such that $s(t_1) = \bar{s}$. Suppose not, i.e. assume that $s(t) \to s^* \geqslant \bar{s}$. Then there are no impulses. So the orbit behaves precisely the same as the orbit of the associated system (3) with initial conditions $(x(0), s(0))$. From the phase portrait of (3), it follows immediately that $\bar{s} < s^* < \lambda$. Since $x(t) \to 0$ as $t \to \infty$, by (5),

$$\begin{aligned} 0 = \lim_{t\to\infty} x(t) &= x(0) + Y\int_{s^*}^{s(0)}\left(1 - \frac{\bar{d}}{f(s)}\right)ds \\ &= x(0) + Y\int_{\mu}^{s(0)}\left(1 - \frac{\bar{d}}{f(s)}\right)ds + Y\int_{s^*}^{\mu}\left(1 - \frac{\bar{d}}{f(s)}\right)ds \\ &= x(\hat{t}) + Y\int_{s^*}^{\mu}\left(1 - \frac{\bar{d}}{f(s)}\right)ds \\ &\geqslant x(\hat{t}) + Y\int_{\bar{s}}^{\bar{s}^+}\left(1 - \frac{\bar{d}}{f(s)}\right)ds \\ &= x(\hat{t}) + D_{\bar{s}} \\ &> 0, \qquad \text{since } \ x(\hat{t}) > 0 \ \text{ and } \ D_{\bar{s}} \geqslant 0, \end{aligned}$$

a contradiction. Hence there is a finite t_1 such that $s(t_1) = \bar{s}$. By (5),

$$
\begin{aligned}
&x(0)+\quad Y\int_{\bar{s}}^{s(0)}\left(1-\frac{\bar{d}}{f(s)}\right)ds\\
=&x(0)+Y\int_{\mu}^{s(0)}\left(1-\frac{\bar{d}}{f(s)}\right)ds+Y\int_{\bar{s}}^{\mu}\left(1-\frac{\bar{d}}{f(s)}\right)ds\\
=&x(\hat{t})+Y\int_{\bar{s}}^{\mu}\left(1-\frac{\bar{d}}{f(s)}\right)ds\\
>&Y\int_{\bar{s}}^{\mu}\left(1-\frac{\bar{d}}{f(s)}\right)ds\\
=&Y\int_{\bar{s}}^{\bar{s}^+}\left(1-\frac{\bar{d}}{f(s)}\right)ds-Y\int_{\mu}^{\bar{s}^+}\left(1-\frac{\bar{d}}{f(s)}\right)ds\\
=&Y\int_{\bar{s}}^{\bar{s}^+}\left(1-\frac{\bar{d}}{f(s)}\right)ds+Y\int_{\mu}^{\bar{s}^+}\left(\frac{\bar{d}}{f(s)}-1\right)ds\\
=&D_{\bar{s}}+D^{\mu}\geqslant\frac{D^{\mu}}{1-r}.
\end{aligned}
$$

Hence (A_3) holds. □

Proof of Theorem 2.2.

Proof. Since the associated system (3) does not admit periodic orbits, any periodic orbit of (1) must have at least one impulse, i.e. it must reach $\bar{s}$ at least once in each cycle.

Suppose that $(x(t),s(t))$ is a T-period orbit of (1) with $k>1$ impulses per period. Without loss of generality, assume that $s(0)=\bar{s}^+$. Then $t_k=T$, and at the impulse times $t_1,t_2,\cdots,t_k$, $x(t_1^-)\neq x(t_2^-)\neq x(t_3^-)\neq\cdots\neq x(t_k^-)$, but $x(t_{k+1}^-)=x(t_1^-)$. By Lemma 5.6,

$$x(t_{k+1}^-)=\frac{1}{r}D_{\bar{s}}+(1-r)^k\left(x(t_1^-)-\frac{1}{r}D_{\bar{s}}\right).$$

Setting $x(t_{k+1}^-)=x(t_1^-)$, and simplifying it follows that $x(t_1^-)=\frac{1}{r}D_{\bar{s}}$, and for $i=2,3,\cdots,k$

$$x(t_i^-)=\frac{1}{r}D_{\bar{s}}+(1-r)^{i-1}\left(x(t_1^-)-\frac{1}{r}D_{\bar{s}}\right)=\frac{1}{r}D_{\bar{s}}.$$

contradicting the assumption that $x(t_1^-)\neq x(t_2^-)\neq\cdots\neq x(t_k^-)$. Therefore, any periodic orbit $(x(t),s(t))$ of (1) must have exactly one impulse each period.

Next, assume $\frac{1-r}{r}D_{\bar{s}}\leqslant D^{\mu}$. Let $(x(t),s(t))$ be a T-periodic solution of (1). Since any periodic orbit must have exactly one impulse per period, without loss of generality, assume that $s(0)=\bar{s}^+$ and so $t_1=T$, where $s(T^-)=\bar{s}$. From the impulsive conditions in (1), $s(T^+)=\bar{s}^+$ and $x(T^+)=(1-r)x(T^-)$. Since the solution is T-periodic, $s(0^+)=s(T^+)=\bar{s}^+$ and $x(0^+)=x(T^+)$. Therefore, $x(T^-)=\frac{1}{1-r}x(0^+)$. From (5),

$$\frac{1}{1-r}x(0^+)=x(T^-)=x(0^+)+Y\int_{s(T^-)}^{s(0^+)}\left(1-\frac{\bar{d}}{f(s)}\right)ds=x(0^+)+D_{\bar{s}}.$$

Therefore,

$$x(0^+) = \frac{1-r}{r} D_{\bar{s}}.$$

$$\begin{aligned} x(T^+) &= (1-r)x(T^-) = (1-r)\left(x(0^+) + D_{\bar{s}}\right) \\ &= (1-r)\left(\frac{1-r}{r} D_{\bar{s}} + D_{\bar{s}}\right) = \frac{1-r}{r} D_{\bar{s}} \leqslant D^\mu. \end{aligned}$$

Using initial condition $(x(T^+), s(T^+))$, (A_2) is not satisfied, and so by case i) in Lemma 5.4, it follows that $s(t) > \mu$ for all finite $t > T$, which contradicts the assumption that $(x(t), s(t))$ is a periodic orbit of (1). Thus, if a periodic orbit exists, $\frac{1-r}{r} D_{\bar{s}} > D^\mu$.

Suppose $\frac{1-r}{r} D_{\bar{s}} > D^\mu$. We show that a nontrivial periodic orbit exists. Consider the orbit $(x(t), s(t))$ of (3) with $s(0) = \bar{s}^+$ and $x(0) = \frac{1-r}{r} D_{\bar{s}} > D^\mu$.

$$\begin{aligned} x(0) + &\quad Y \int_\mu^{s(0)} \left(1 - \frac{\bar{d}}{f(s)}\right) ds \\ =& \frac{1-r}{r} D_{\bar{s}} - Y \int_\mu^{\bar{s}^+} \left(\frac{\bar{d}}{f(s)} - 1\right) ds \\ =& \frac{1-r}{r} D_{\bar{s}} - D^\mu > D^\mu - D^\mu = 0. \end{aligned}$$

Hence (A_2) is satisfied. Since $f(s) < \bar{d}$ for $\bar{s}^+ > \mu$, $D^\mu > 0$. Also, $\frac{1-r}{r} D_{\bar{s}} > D^\mu$ implies that $D_{\bar{s}} > 0$. Then

$$\begin{aligned} x(0) + &\quad Y \int_{\bar{s}}^{s(0)} \left(1 - \frac{\bar{d}}{f(s)}\right) ds \\ =& x(0) + Y \int_{\bar{s}}^{\bar{s}^+} \left(1 - \frac{\bar{d}}{f(s)}\right) ds \\ =& \frac{1-r}{r} D_{\bar{s}} + D_{\bar{s}} = \frac{1}{r} D_{\bar{s}} > 0. \end{aligned}$$

Therefore, (A_1) is satisfied. By Lemma 5.2*iii)*, there exists an impulse time $t_1 > 0$, finite, such that $s(t_1^-) = \bar{s}$ and $x(t_1^-) > 0$. Thus we have shown that if $\frac{1-r}{r} D_{\bar{s}} > D^\mu$, this orbit has at least one impulse at time t_1.

Next, we show that this orbit is periodic of period t_1. By (5),

$$\begin{aligned} x(t_1^-) &= x(0) + Y \int_{s(t_1^-)}^{s(0)} \left(1 - \frac{\bar{d}}{f(s)}\right) ds \\ &= x(0) + Y \int_{\bar{s}}^{\bar{s}^+} \left(1 - \frac{\bar{d}}{f(s)}\right) ds \\ &= \frac{1-r}{r} D_{\bar{s}} + D_{\bar{s}} = \frac{1}{r} D_{\bar{s}} > 0. \end{aligned}$$

By the impulse conditions (1),

$$\begin{aligned} x(t_1^+) &= x(t_1^-) - r x(t_1^-) = (1-r)x(t_1^-) = \frac{1-r}{r} D_{\bar{s}} = x(0) \\ s(t_1^+) &= s(t_1^-) - r\bar{s} + r s^i = (1-r)\bar{s} + r s^i = \bar{s}^+ = s(0). \end{aligned}$$

Therefore, there is a periodic orbit of (1) if and only if $\frac{1-r}{r} D_{\bar{s}} > D^\mu$.

To show the uniqueness of the periodic orbit (up to translation in time), without loss of generality, let $s(0^+) = \bar{s}^+$ so that $s(T^-) = \bar{s}$ and $s(T^+) = \bar{s}^+$. By (5), $x(T^-) = x(0^+) + D_{\bar{s}}$. But, on a periodic orbit with one impulse per cycle, $x(0^+) = x(T^+) = (1-r)x(T^-)$, and so $x(T^-) = \frac{1}{r}D_{\bar{s}}$.

Hence, there is a unique periodic orbit. Clearly, at the impulse points, the periodic orbit satisfies $s(t_n^-) = s(T^-) = \bar{s}$, $s(t_n^+) = s(0^+) = \bar{s}^+$, $x(t_n^-) = x(T^-) = \frac{1}{r}D_{\bar{s}}$, and $x(t_n^+) = x(0^+) = \frac{1-r}{r}D_{\bar{s}}$.

As in [23] we can apply impulsive Floquet theory to system (1) to establish orbital asymptotic stability of the periodic orbit and asymptotic phase. The calculation is identical to that given in [23] where it is shown that the nontrivial multiplier is equal to $1-r$ and so lies inside the unit circle. The expression for T was also derived in [23]. □

Proof of Theorem 2.3.

Proof. 1. Since $\frac{1-r}{r}D_{\bar{s}} > D^{\mu}$, by Theorem 2.2, there exists a unique asymptotically stable periodic orbit with positive period $T > 0$. See Figure 3 (TOP).

1. i) First, assume that (A_3) is satisfied and $s(0) \leqslant \mu$. Since (A_3) holds, (A_1) holds and so by Lemma 5.2*ii)*, there exists a $t_1 > 0$, finite, such that $s(t_1) = \bar{s}$ and $x(t_1^-) > 0$. By Lemma 5.5, there exists an infinite sequence of impulse times $\{t_n\}_{n=1}^{\infty}$ such that $s(t_n^-) = \bar{s}$, $s(t_n^+) = \bar{s}^+$ (and $x(t_n^+) > D^{\mu}$). By Lemma 5.6, $x(t_n^-) \to \frac{1}{r}D_{\bar{s}}$ and $x(t_n^+) \to \frac{1-r}{r}D_{\bar{s}}$ as $n \to \infty$. Therefore, this orbit converges to the periodic orbit.

Next, assume that (A_2) holds and $s(0) > \mu$. By Lemma 5.7, (A_3) also holds, and hence (A_1) holds (since $D^{\mu} \geqslant 0$ and $r \in (0,1)$). By Lemma 5.2*iii)*, there exists a $t_1 > 0$, finite, such that $s(t_1) = \bar{s}$ and $x(t_1^-) > 0$. The proof that the orbit converges to the periodic orbit now follows as in the previous paragraph using Lemmas 5.5 and 5.6.

1. ii) Since $s(0) \leqslant \mu$ and (A_1) is satisfied, by Lemma 5.2*ii)*, there exists a $t_1 > 0$, finite, such that $s(t_1) = \bar{s}$ and $x(t_1^-) > 0$. Since (A_3) is violated, by Lemma 5.5, $s(t) > \mu$ for all finite $t > t_1$, and $s(t) \to s^* \geqslant \mu$, $x(t) \to 0$ as $t \to \infty$.

1. iii) First assume that $s(0) \leqslant \mu$ and (A_1) is not satisfied. It follows that $\bar{s} < \lambda$. By Lemma 5.3, $s(t) > \bar{s}$ for all finite t and $s(t) \to s^* \geqslant \bar{s}$ as $t \to \infty$. From the vector field it is clear that $s^* < \lambda$.. Next assume that $s(0) > \mu$ and (A_2) is not satisfied. The result follows by Lemma 5.4*i)*.

1. i) a) If $x(t_1^-) = \frac{1}{r}D_{\bar{s}}$, then by the impulse condition for system (1), $x(t_n^+) = \frac{1-r}{r}D_{\bar{s}}$ and we are on the periodic orbit.

1. i) b) If $x(t_1^-) < \frac{1}{r}D_{\bar{s}}$, by Lemma 5.6,

$$x(t_n^-) < x(t_{n+1}^-) < \frac{D_{\bar{s}}}{r}, \qquad \text{for} \qquad n = 1, 2, 3, \cdots,$$

$$x(t_n^+) < x(t_{n+1}^+) < \frac{(1-r)}{r}D_{\bar{s}}, \qquad \text{for} \qquad n = 1, 2, 3, \cdots.$$

By Lemma 5.1, $t_n - t_{n-1} > t_{n+1} - t_n > T$.

1.i) c) If $x(t_1^-) > \frac{1}{r}D_{\bar{s}}$, the proof follows by reversing the inequalities in the previous case.

2. Assume that $\frac{1-r}{r}D_{\bar{s}} = D^{\mu}$. By Theorem 2.2, no periodic orbit exists. We show that instead, the critical curve plays the role of the periodic orbit in case *1*, but with infinite period. see Figure 3 (MIDDLE).
2. i) Assume that the initial conditions satisfy $s(0) \leqslant \mu$ and (A_3), or $s(0) > \mu$ and (A_2). As in the proof of *1.i)*, by Lemma 5.2 and Lemma 5.5, there are an infinite number of impulses $\{t_n\}_{n=1}^{\infty}$ such that $s(t_n^-) = \bar{s}$, $s(t_n^+) = \bar{s}^+$ and $x(t_n^+) > D^{\mu}$. By Lemma 5.6, $x(t_n^-) \to \frac{1}{r}D_{\bar{s}}$ and $x(t_n^-) \to \frac{1-r}{r}D_{\bar{s}}$ as $n \to \infty$, with sequences $\{x(t_n^+)\}$ and $\{x(t_n^+)\}$ each decreasing monotonically. The sequence $\{\eta_n\} = \{x(t_n^+) - D^{\mu}\} \to 0$ as $n \to \infty$ and so by Lemma 5.1 the orbit undergoes an infinite number of impulses and converges to the critical curve. Thus, there is a sequence of times $\{\tau_n\} \to \infty$ as $n \to \infty$ with $(x(\tau_n), s(\tau_n)) \to (0, \mu)$. Therefore, $\liminf_{t\to\infty} x(t) = 0$. Also, the period of the orbits increases and approaches the period of the critical curve. However, the critical curve is not actually an orbit, but rather is made up of the equilibrium point $(0, \mu)$ and its stable and unstable manifolds. Any orbit starting at $(D^{\mu}, \bar{s}^+)$ (on the critical curve), takes an infinite amount of time to reach the equilibrium point $(0, \mu)$, and hence the closer the orbit gets to the critical curve, after each impulse the longer it takes to reach $\bar{s}$, with the time between impulses approaching infinity.

2. ii) The proof is the same as in case *1. ii)*

2. iii) The proof is the same as in case *1. iii)*.

3. Assume that $\frac{1-r}{r}D_{\bar{s}} < D^{\mu}$. By Theorem 2.2, system (1) admits no periodic orbit. See Figure 3 (BOTTOM).

To show there are at most a finite number of impulses, we use proof by contradiction. Suppose there exists an infinite sequence of distinct impulse times $\{t_n\}_{n=1}^{\infty}$ such that $s(t_n^-) = \bar{s}, s(t_n^+) = \bar{s}^+$ and $x(t_n^+) > 0$. If $x(t_1^+) \leqslant \frac{1-r}{r}D_{\bar{s}}$, then $x(t_1^+) < D^{\mu}$ and so (A_2) is not satisfied. By Lemma 5.4*i)* $s(t) > \mu$ for all finite $t > t_1$. This contradicts $s(t_n^+) = \bar{s}^+ < \mu$ for $n > 1$.

If $x(t_1^+) > \frac{1-r}{r}D_{\bar{s}}$, by Lemma 5.6, $x(t_n^+) > \frac{1-r}{r}D_{\bar{s}}$ for all positive integers n and $x(t_n^+) \to \frac{1-r}{r}D_{\bar{s}}$ as $n \to \infty$. Hence, for some sufficiently large k, $x(t_k^+) < D^{\mu}$ and (A_2) is violated. The result follows by Lemma 5.4. □

Proof of Theorem 2.4.

Proof. Since $\mu \leqslant \bar{s} < \bar{s}^+$ and $f(s) < \bar{d}$ for $s > \mu$, it follows that $D^{\mu} > 0$ and $D_{\bar{s}} < 0$. Therefore, $\frac{1-r}{r}D_{\bar{s}} < D^{\mu}$. If (A_1) is not satisfied, the result follow by Lemma 5.3. If (A_1) is satisfied, then by Lemma 5.2*i)*, there exists a $t_1 > 0$, finite, such that $s(t_1^-) = \bar{s}$ and $x(t_1^-) > 0$. Suppose there exists an infinite number of impulse times $\{t_n\}_{n=1}^{\infty}$ such that $s(t_n^-) = \bar{s}$. By Lemma 5.6, $x(t_n^-) \to \frac{1}{r}D_{\bar{s}} < 0$ as $n \to \infty$. So there exists an integer k such that $x(t_k^-) < 0$. Since this is impossible, there are at most a finite number of impulses. □

Proof of Theorem 4.1.

Proof. So that the fermentor cycles indefinitely without the time between impulses becoming unbounded, by Theorem 2.3, in order for $r \in (r_0, r^0)$, it is necessary to ensure that $\frac{(1-r)}{r}D_{\bar{s}}(r) > D^{\mu}(r)$, and hence that $D_{\bar{s}}(r) > 0$.

$$\frac{d}{dr}D_{\bar{s}}(r) = Y(s^i - \bar{s})\left(1 - \frac{\bar{d}}{f(\bar{s}^+)}\right). \tag{15}$$

$$\frac{d}{dr}D^{\mu}(r) = \begin{cases} 0, & \bar{s}^{+} \leqslant \mu, \\ Y(s^{i}-\bar{s})\left(\frac{\bar{d}}{f(\bar{s}^{+})}-1\right) > 0, & \bar{s}^{+} > \mu. \end{cases}$$

Therefore, if $\bar{s}^{+} \in (\lambda,\mu)$, then $\frac{d}{dr}D_{\bar{s}}(r) > 0$, but if $\bar{s}^{+} \in [0,\lambda]\cup[\mu,\infty]$, $\frac{d}{dr}D_{\bar{s}}(r) < 0$. Thus,

$$\begin{array}{lllll} \frac{d}{dr}D_{\bar{s}}(r) < 0, & \text{for} & & r & < \frac{\lambda-\bar{s}}{s^{i}-\bar{s}}, \\ \frac{d}{dr}D_{\bar{s}}(r) > 0, & \text{for} & \frac{\lambda-\bar{s}}{s^{i}-\bar{s}} & < r & < \frac{\mu-\bar{s}}{s^{i}-\bar{s}}, \\ \frac{d}{dr}D_{\bar{s}}(r) < 0, & \text{for} & \frac{\mu-\bar{s}}{s^{i}-\bar{s}} & < r. & \end{array}$$

Since $D_{\bar{s}}(0) = 0$, either $D_{\bar{s}}(r) < 0$ for all $r \in (0,1)$, and there is no choice of r that would result in successful operation, or there exists an interval $(r_0,r_1) \subseteq [0,1]$ such that $D_{\bar{s}}(r_0) = 0$, $(1-r_1)D_{\bar{s}}(r_1) = 0$, and $D_{\bar{s}}(r) > 0$ when $r \in (r_0,r_1)$, where $\max\{\frac{\lambda-\bar{s}}{s^{i}-\bar{s}},0\} \leqslant r_0 < \frac{\mu-\bar{s}}{s^{i}-\bar{s}}$ and $r_0 < r_1 \leq 1$.

If $r = 0$, then $\bar{s} = \bar{s}^{+}$. Since, we are assuming that $\bar{s} < \mu$, for r positive and sufficiently close to 0, $D^{\mu}(r) = 0$. If $\bar{s} < \lambda$, then $\frac{d}{dr}, D_{\bar{s}}(0) < 0$, and since $D_{\bar{s}}(0) = 0$, if r_0 exists, $r_0 > 0$. However, if $\lambda < \bar{s} < \mu$, then $\frac{d}{dr}D_{\bar{s}}(0) > 0$, and $r_0 = 0$.

If $r_0 \in [0,1)$ exists, for $r \in \left(r_0, \frac{\mu-\bar{s}}{s^{i}-\bar{s}}\right]$, $\bar{s}^{+} \leqslant \mu$, and so $D_{\bar{s}}(r) > 0$ and by definition $D^{\mu}(r) = 0$, and hence $\frac{1-r}{r}D_{\bar{s}}(r) > D^{\mu}(r)$.

If $\frac{\mu-\bar{s}}{s^{i}-\bar{s}} \geqslant 1$, i.e., $\mu \geqslant s^{i}$, then $r^{0} = 1$. This would be the case, for example, if the response functions are monotone increasing.

If, on the other hand, $\mu < s^{i}$, then $r_1 > \frac{\mu-\bar{s}}{s^{i}-\bar{s}}$. It follows that for $r \in \left(\frac{\mu-\bar{s}}{s^{i}-\bar{s}}, r_1\right)$, $\bar{s}^{+} > \mu$, and so $\frac{d}{dr}D^{\mu}(r) > 0$, and $\frac{d}{dr}D_{\bar{s}}(r) < 0$. Therefore,

$$\frac{d}{dr}\left((1-r)D_{\bar{s}}(r) - rD^{\mu}(r)\right) < 0 \qquad \text{for} \qquad r \in \left[\frac{\mu-\bar{s}}{s^{i}-\bar{s}}, r_1\right].$$

Since,

$$(1-r)D_{\bar{s}}(r) - rD^{\mu}(r) > 0, \text{ if } r = \frac{\mu-\bar{s}}{s^{i}-\bar{s}} \text{ and } (1-r_1)D_{\bar{s}}(r_1) - r_1D^{\mu}(r_1) < 0,$$

there must exist $r^{0} \in \left[\frac{\mu-\bar{s}}{s^{i}-\bar{s}}, r_1\right]$, with $r^{0} < 1$, such that $(1-r^{0})D_{\bar{s}}(r^{0}) - r^{0}D^{\mu}(r^{0}) = 0$, and

$$(1-r)D_{\bar{s}}(r) - rD^{\mu}(r) > 0 \qquad \text{for} \qquad r \in \left[\frac{\mu-\bar{s}}{s^{i}-\bar{s}}, r^{0}\right).$$

Therefore, once all parameters except r are fixed, if there exists some $r \in (0,1)$ such that $\frac{(1-r)}{r}D_{\bar{s}}(r) > D^{\mu}(r)$, then there exists an interval $[r_0,r^{0}] \subset [0,1]$ such that $\frac{(1-r)}{r}D_{\bar{s}}(r) - D^{\mu}(r) > 0$ for all $r \in (r_0,r^{0})$ and $(1-r^{0})D_{\bar{s}}(r^{0}) - r^{0}D^{\mu}(r^{0}) = 0 = (1-r_0)D_{\bar{s}}(r_0) - r^{0}D^{\mu}(r_0) = 0$. The result follows by Theorem 2.3. □

6. **Discussion.** SCF has many potential applications including water purification, biological waste decomposition, and toxic waste clean up. Keeping these applications in mind, and thinking of the nutrient as a contaminant, we used the acceptable concentration of the contaminant, $\bar{s}$, as the triggering mechanism and studied nutrient driven SCF. A safe level for $\bar{s}$ is often set by an environmental protection agency and so $\bar{s}$ must be chosen at or below this acceptable concentration. For example, in the water purification process, $\bar{s}$ must be set so that the water meets the appropriate standard to ensure that it is safe for drinking.

Some contaminants (such as phenols, thiocyanate, nitrites, etc.) in industrial or toxic waste are inhibitory to many of the microorganisms metabolizing them

at higher concentrations. In our model, we consider response functions that are unimodal to model this inhibitory effect at high concentrations, thus generalizing the model considered in [23] where only monotone increasing response functions were considered.

Our model predicts that if $\frac{1-r}{r}D_{\bar{s}} > D^{\mu}$, then there are appropriate initial conditions for which the fermentor cycles indefinitely with bounded cycle time, but that the process fails otherwise. (In the case of monotone response functions, (see [23]) success depends upon whether $D_{\bar{s}} > 0$.) When the process fails, either there are at most a finite number of cycles and then the threshold level of contaminant $\bar{s}$ is never again met, or the tank cycles indefinitely, but the time between cycles becomes unbounded. Even in this latter case, during each cycle, there are times when the concentration of microorganisms becomes so small, that in actual experiments, it is more likely that the cycling eventually stops.

For a particular choice of microorganisms, the response function $f(s)$ and the death rate $\bar{d}$, and hence the break-even parameters λ and μ are no longer under the control of the experimenter. As well, the concentration of the contaminant in the medium used to refill the tank is also usually fixed, as is the maximum safe level of this contaminant, $\bar{s}$. However, r the emptying/refilling fraction remains under the control of the experimenter and $D_{\bar{s}}$ and D^{μ} depend on r. D^{μ} is an increasing function of r. See (15) for the dependence of $D_{\bar{s}}$ on r. $D_{\bar{s}}$ attains its maximum value at $r = \min(\frac{\mu-\bar{s}}{s^i-\bar{s}}, 1)$. If this maximum value is negative, then no choice for r would result in successful operation of the fermentor and a different population of microorganisms would have to be used. However, if it is positive, then there exists an interval $(r_0, r^0) \subset [0,1]$ where $\frac{1-r}{r}D_{\bar{s}}(r) > D^{\mu}(r)$, and, at least in theory, the process can succeed provided appropriate initial conditions are chosen. If $\mu > \bar{s} \geqslant \lambda$, then $r_0 = 0$, otherwise $r_0 > 0$. If $\mu \geqslant s^i$, then $r^0 = 1$, otherwise $r_0 < \frac{\mu-\bar{s}}{s^i-\bar{s}} < r^0$.

It is often important in applications to optimize the yield, i.e., the total volume of medium processed over some fixed time. It was shown that this yield depends continuously on the emptying/refilling fraction. If the emptying/refilling fraction r falls outside (r_0, r^0), the process terminates after at most a finite number of cycles. (In the case of monotone response functions, $r^0 = 1$.) If the emptying/refilling fraction r falls in this interval, but too close to r_0 or r^0, the process could still fail in practice, because the microorganisms fail to reduce the contaminant to an acceptable concentration in a reasonable amount of time between cycles. Simulations of the model predict that over all successful choices of emptying/refilling fractions, there exists an optimal emptying/refilling fraction $r \in (r_0, r^0)$, at which the yield over a fixed time is maximized. Based on an explicit formula for the eventual cycle time, we showed how to choose the optimal emptying/refilling fraction and how to calculate the maximum yield, once all parameters except the emptying/refilling fraction are fixed.

Although the maximum value for $\bar{s}$ cannot be violated in such applications as water purification, using a smaller value for $\bar{s}$ would only result in cleaner water. However, one would expect that the larger the choice for $\bar{s}$, the more water could be processed and hence the more economical. A surprising implication of our results is that, if for a particular population of microorganisms, the acceptable level of the contaminant $\bar{s}$ is greater than μ, the process always fails, no matter the choice of r. However, it is possible to make the process succeed, by actually reducing $\bar{s}$. For example, by setting $\bar{s} = \lambda$ one can choose $r \in (0,1)$ so that $\bar{s}^+ = \mu$. Then, $D_{\bar{s}} > 0$

and there are initial conditions for which the process is successful. One could then try to find better choices for $\bar{s} \in [\lambda, \mu)$ and r that optimize the yield.

Once an appropriate value of r is selected for which $\frac{1-r}{r} D_{\bar{s}} > D^{\mu}$, so that the process has a chance to succeed, it is still necessary to choose appropriate initial concentrations of the contaminant and the microorganisms (see Figure 3 (TOP)). If $\bar{s}^{+} \leqslant \mu$ then one only needs to ensure that the initial conditions satisfy (A_1), i.e., the region bounded by the dash-dotted curve is avoided. If $\bar{s}^{+} > \mu$ then one needs to ensure that (A_2) and (A_3) are satisfied, i.e., that when $s(0) \geqslant \mu$, the orbit starts in the region to the right of the dashed curve, and when $s(0) < \mu$, the orbit starts in the region above and to the right of the dotted curve.

Usually, one would expect $s(0) = s^{i}$. If $\bar{s}^{+} > \mu$, failure of the system can be prevented by diluting the medium before the first cycle. This is particularly useful if the microorganisms are scarce or expensive. For example, if $\frac{1-r}{r} D_{\bar{s}} > D^{\mu}$ as in Figure 3 (TOP), but $s(0) \geqslant \bar{s}^{+} > \mu$ and the orbit starts in the region to the left of the dashed curve, the process terminates without a single impulse. However, diluting the medium (i.e., decreasing $s(0)$) so that the orbit starts in the region to the right of the dashed curve, or even between the dotted and the dashed curves, results in success. But, diluting too much, so that the orbit starts in the region below and to the left of the dotted curve again results in failure.

Although diluting the contaminated medium before the first cycle can be effective, it would not be effective to dilute the medium before each cycle, since it would be more efficient to reduce r. Reducing r results in a shorter cycle time than diluting, since it leaves more processed medium with a higher concentration of microorganisms in the tank to process the medium, and it cuts down on the time taken for emptying and refilling. Therefore, dilution before every cycle cannot improve upon the result obtained using the optimal value of r.

When the process is successful in the sense that it cycles indefinitely with reasonable cycle time, the level of microorganisms released is eventually very close to $\frac{1}{r} D_{\bar{s}}$. The population of microorganisms must be chosen so that this level is safe. If the microorganisms are inexpensive and not toxic at even higher levels, the higher the concentration of microorganisms used to initiate the process, the better. Our analysis predicts that the larger the initial concentration of microorganisms, the faster the acceptable level of contaminant, $\bar{s}$ is reached during the initial cycles (before the periodic cycle is reached). Actually to speed up the process, it is helpful to add microorganisms whenever possible, say, at the start of every cycle, provided the concentration of the microorganisms at each impulse time is safe.

If one has several potential strains to choose from, it does not seem to be the strains that have the highest specific growth rate over the largest range of concentration of the contaminant, but rather the ones that have the highest specific growth rate over very low concentrations of the contaminant, close to the threshold $\bar{s}$, that appear to be the most efficient. (See Figures 4 and 8).

A discussion of the advantages of SCF over the chemostat for such applications as water purification and toxic waste clean up was given in [23]. In particular, based on the analysis in [11, 28], it was explained that certain strains of microorganisms could be used successfully for SCF that would fail if used in the chemostat. In particular, for all four strains considered in this paper, the chemostat could not be used since $f(\bar{s}) < \bar{d}$, and so no dilution rate could be chosen for which the chemostat could reduce the level of the contaminant to the acceptable level $\bar{s}$. If a strain was found for which $f(\bar{s}) > \bar{d}$, then both processes have the potential to succeed and it would

be interesting to determine which process would be more efficient. However, SCF still has the advantage that if the strain of microorganisms undergoes mutation, the level of the contaminant released would never become unsafe, whereas this might not be the case for the chemostat.

Acknowledgements. The authors would like to thank the anonymous referees for their valuable suggestions. This research is based in part on the first authors's M.Sc. thesis at McMaster University.

REFERENCES

[1] S. Aiba, M. Shoda and M. Nagatani, *Kinetics of product inhibition in alcohol kinetics*, Biotechnol. Bioeng., **10** (2003), 845–864.
[2] G. Alagappan and R. M. Cowan, *Biokinetic models for representing the complete inhibition of microbial activity at high substrate concentrations*, Biotechnol. Bioeng., **75** (2001), 393–405.
[3] G. Alagappan and R. Cowan, *Substrate inhibition kinetics for toluene and benzene degrading pure cultures and a method for collection and analysis of respirometric data for strongly inhibited cultures*, Biotechnol. Bioeng., **83** (2003), 798–809.
[4] J. F. Andrews, *A mathematical model for the continuous culture of microorganisms utilizing inhibitory substrates*, Biotechnol. Bioeng., **10** (1968), 707–723.
[5] D. D. Bainov and P. S. Simeonov, "Systems with Impulsive Effect," Ellis Horwood Ltd, Chichester, 1989.
[6] D. D. Bainov and P. S. Simeonov, "Impulsive Differential Equations: Periodic Solutions and Applications," Longman Scientific and Technical, Burnt Mill, 1993.
[7] D. D. Bainov and P. S. Simeonov, "Impulsive Differential Equations: Asymptotic Properties of the Solutions," World Scientific, Singapore, 1995.
[8] B. Boon and H. Laudelout, *Kinetics of nitrite oxidation by nitrobacter winogradskyi*, Biochem. J., **85** (1962), 440–447.
[9] W. A. Brown and D. G. Cooper, *Self-cycling fermentation applied to acinetobacter calcoaceticus RAG-1*, Appl. Environ. Microbiol., **57** (1991), 2901–2906.
[10] W. A. Brown and D. G. Cooper, *Hydrocarbon degradation by Acinetobacter calcoaceticus RAG-1 using the self-cycling fermentation technique*, Biotechnol. Bioeng., **40** (1992), 797–805.
[11] G. J. Butler and G. S. K. Wolkowicz, *A mathematical model of the chemostat with a general class of response functions describing nutrient uptake*, SIAM J. Appl. Math., **45** (1985), 138–151.
[12] V. H. Edwards, *The influence of high substrate concentrations on microbial kinetics*, Biotechnol. Bioeng., **12** (1970), 679–712.
[13] F. B. Godin, D. G. Cooper and A. D. Rey, *Development and solution of a cell mass population balance model applied to the SCF process*, Chem. Eng. Sci., **54** (1999), 565–578.
[14] J. B. S. Haldane, "Enzymes," Longmans, Green and Co. Ltd, London, Great Britain, 1930, (Reprinted in 1965 by the Massachusetts Institute of Technology).
[15] V. Lakshmikantham, D. D. Bainov and P. S. Simeonov, "Theory of Impulsive Differential Equations," World Scientific, Singapore, 1989.
[16] J. H. T. Luong, *Generalization of Monod kinetics for analysis of growth data with substrate inhibition*, Biotechnol. Bioeng., **29** (1987), 242–248.
[17] A. Novick and L. Szilard, *Description of the chemostat*, Sci., **112** (1950), 715-716.
[18] E. O. Powell, *Theory of the Chemostat*, Lab. Pract., **14** (1965), 1145–1149.
[19] B. E. Sarkis and D. G. Cooper, *Biodegradation of aromatic compound in a self-cycling fermenter (SCF)*, Can. J. Chem. Eng., **72** (1994), 874–880.
[20] J. D. Sheppard and D. G. Cooper, *Development of computerized feedback control for the continuous phasing of Bacillus subtilis*, Biotechnol. Bioeng., **36** (1990), 539–545.
[21] R. J. Smith, "Impulsive Differential Equations with Applications to Self-cycling Fermentation," PhD thesis, McMaster University, 2001.
[22] R. J. Smith and G. S. K. Wolkowicz, *A size-structured model for the nutrient-driven self-cycling fermentation process*, Dyn. Contin. Discrete Impuls. Syst. Ser. B Appl. Algorithms, **10** (2003), 207–219.

[23] R. J. Smith and G. S. K. Wolkowicz, *Analysis of a model of the nutrient driven self-cycling fermentation process*, Dyn. Contin. Discrete Impuls. Syst. Ser. B Appl. Algorithms, **11** (2004), 239–265.
[24] R. J. Smith and G. S. K. Wolkowicz, *Coexistence of competing species in nutrient driven self-cycling fermentation*, preprint.
[25] M. Wayman, and M. C. Tseng, *Inhibition-threshold substrate concentrations*, Biotechnol. Bioeng., **18** (1976), 383–387.
[26] S. D. Wentworth and D. G. Cooper, *Self-cycling fermentation of a citric acid producing strain of Candida lipolytica*, J. Ferment. Bioeng., **81** (1996), 400-405.
[27] B. M. Wincure, D. G. Cooper and A. Rey, *Mathematical model of self-cycling fermentation*, Biotechnol. Bioeng., **46** (1995), 180–183.
[28] G. S. K. Wolkowicz and Z. Lu, *Global dynamics of a mathematical model of competition in the chemostat: general response functions and differential death rates* SIAM J. Appl. Math., **52** (1992), 222–233.
[29] M. G. Zenaitis and D. G. Cooper, *Antibiotic production by Streptomyces aureofaciens using self-cycling fermentation*, Biotechnol. Bioeng., **44** (1994), 1331–1336.

Received January 2007; revised May 2007.

E-mail address: gfan@math.mcmaster.ca
E-mail address: wolkowic@mcmaster.ca